
Università degli Studi di Padova

Dipartimento di Fisica e Astronomia "Galileo Galilei"

Corso di Laurea Magistrale in

Astronomia

# THE IMPACT OF BINARY STARS IN THE DETERMINATION OF THE TOTAL MASS OF STELLAR SYSTEMS

**Relatore:** Giovanni Carraro
**Contro-relatore:** Michela Mapelli

**Laureanda:** Camilla Pianta

"One, remember to look up in the sky and not down on your feet. Two, never give up work. Work gives you meaning and purpose and life is empty without it. Three, if your are lucky enough to find love, remember it is there and don't throw it away."

*Stephen Hawking*

**Abstract**

Binary stars play a very important role in the dynamics of stellar systems such as star clusters. After a detailed analysis of binary classification, formation mechanisms and both fundamental parameters and distributions, the impact of binaries in the determination of the total cluster mass has been investigated by means of *N*-body simulations founded on the code *NBODY7*. Since the primordial binary fraction is a crucial ingredient in star cluster dynamical evolution, three open-clusters-like models characterised by a different initial binary percentage have been realised and a careful examination of their outputs has been performed. In the end, two HRD-based methods, i.e. the photometric and the isochrone fitting methods, have been employed to point out the fact that either neglecting the presence of binaries or not accounting for them properly leads to definitely wrong mass estimates.

# Contents

# Chapter I

# Introduction

## 1.1 Brief historical overview about the discovery of binary stars

The discovery of the first binary stars dates back to the latter part of the $17^{th}$ century. In fact, binary stars were found merely by accident and were initially referred to as "double stars" because the resolution of the telescopes used at that time was too low to properly investigate such systems. As a consequence, astronomers believed that a binary system consisted simply of two stars seen nearly at the same line of sight, but not physically connected, and probably very distant from each other. In particular, this was thought to be the case of binary systems where one star was considerably brighter than the companion.

The first discovered binary system was Mizar (1650), which was followed by $\gamma$ Arietis (1664), $\alpha$ Crucis (1685) and $\alpha$ Centauri (1689).

The so called double stars were then carefully observed in order to obtain precise measurements of the stellar parallax: this was their main use in astronomy before they were recognised as stars interacting and affecting each other in their physical evolution. It was only in 1787 that the astronomer John Mitchell advanced the hypothesis of these stars to be physically connected: that was the starting point of the study of double stars as binary stars.

In the late $18^{th}$ century, Christian Mayer published the first catalog of binary stars (*Christian Mayer's Catalogue Of Double Stars*, 1781), and Sir William Hershel definitely proved that double stars were effectively linked by physical processes when he found that an exchange in their relative position could not be interpreted as a parallactic

displacement (*Catalogue of Double Stars*, 1784). Then Professor Sherburne Burnham, who discovered as many as 1340 binary stars (*Burnham Double Star Catalogue*, 1906), played the role of forerunner for Robert Grant Aitken, an astronomer of the Lick Observatory who gave a huge contribution to the study of binary systems (*The Binary Stars*, 1936).

In particular, now two stars are considered to be a binary system if they obey to the relation:

$$\log(R) < 2.8 - 0.2m \tag{1.1}$$

where $R$ is the distance between the components and $m$ the total apparent magnitude.

The interest in the characterisation and physical analysis of binary stars has grown stronger in the last 30 years thanks to the recognition not only of their impact on stellar evolution, but also of their influence in the dynamics of stellar systems, such as globular and open clusters. For these reasons nowadays binary stars are thought to be fundamental objects to take into account for a proper understanding of the dynamical processes governing stellar physics.

## 1.2 Types of binary stars

Binary stars are usually divided in four different classes according to both the way in which they are discovered and the techniques employed for their study:

- **Visual binaries.**
  A binary system is visual if both its components can be observed by means of a telescope; in such systems the primary is typically brighter than the secondary.

  There are two different methods to investigate visual binaries, i.e. the classical and the interferometric methods. In particular, the former consists in the determination of the seven elements of the binary relative orbit either analytically (Kowalsky method) or grafically (Zwier method); once the semi-major axis of the orbit $a$ is determined and if the distance of the examined binary system is known, the masses of both the components can be derived by using Kepler's third law.

- **Spectroscopic binaries.**
  A binary system is spectroscopic if its components are not resolved and its duplicity has to be inferred through the spectral analysis. In fact, the spectrum of the observed star shows periodic radial velocity variations due to the Doppler effect, which causes the spectral lines to move towards the red if the star is approaching (positive radial velocity) or towards the blue if it is departing

(negative radial velocity). Since the radial velocity can assume both positive and negative values during the relative motion of the binary components, emission and absorption lines are forced to oscillate.

Besides, spectroscopic binaries can be either single-lined (SBI), when only the spectrum of the primary is observed, or double-lined (SBII), when this happens for both stars instead.

- **Photometric (or eclipsing) binaries.**
  A binary system is photometric if its components are not resolved and the duplicity is deduced from the presence of periodic minima in the light curve, each minimum corresponding to an eclipse. Since photometric binaries can be regarded as spectroscopic binaries having an inclination angle $i \simeq 90°$, the line of sight is contained in the orbital plane, so that at every revolution one component is seen to partially or completely eclipse the other.

  In particular, photometric binaries can be distinguished according to the appearance of their light curve, which displays the luminosity variation of one component as a function of its position with respect to the companion:

  – Type 1 photometric binaries.
    As type 1 photometric binaries are spherical-shaped, so that they exhibit always the same side to the observer, their light curve is characterised by the constancy of the total apparent magnitude outside the eclipses.

  – Type 2 photometric binaries.
    In the light curve of type 2 photometric binaries the total apparent magnitude outside the eclipses is variable for both the stars are not perfectly spherical because of the presence of tidal interactions: as a consequence, their shape is quite elongated, so that they don't show the observer always the same side.

  Moreover, type 1 photometric binaries have larger orbital separations, and thus longer orbital periods, than type 2 photometric binaries.

  In the end, it is worth emphasising the case of close binary systems, in which the gravitational coupling between the components is so strong that the rotation and the revolution periods coincide: therefore such systems move as a rigid body around its barycentre. Stars belonging to them are characterised by frequent interaction phenomena, such as mass transfer through the Roche Lobe Overflow (RLOF) mechanism: if the radius of one component exceeds that of the Roche Lobe, then the mass transfer from one star to the companion gets started. This generally happens during those evolutionary phases in which one star expands, thus increasing its radius (i.e. in the transition from the Main Sequence (MS) to

the Red Giant Branch (RGB)), until it fills its Roche Lobe.
Also, stars experiencing mass transfer are typically sorrounded by a rapidly rotating accretion disk; the material which the disk is made of is lost by the donors together with angular momentum and is meant for the mass accretion of the receiving stars once it settles down to their surface because of the acceleration imprinted by the stellar gravitational field.

Lastly, close binary systems are divided in three groups depending on the behaviour of their components towards the Roche Lobe:

- Detached systems.
  Close binary systems are defined as detached when both their components have $R<R_{RL}$ (i.e. none of them fills its Roche Lobe).
- Semi-detached systems.
  Close binary systems are semi-detached when the primary has $R_1<R_{RL}$, whereas the secondary has $R_2\simeq R_{RL}$ (i.e. only the secondary fills its Roche Lobe); in this case mass transfer from the secondary to the primary is likely to get underway.
- Contact systems.
  Close binary systems belong to this category if both their components have $R\simeq R_{RL}$ (i.e. both of them fill their Roche Lobe), so that sooner or later mass transfer will be initiated.

- **Astrometric binaries.**
  A binary system is astrometric if its components are not resolved and the duplicity is derived by studying the perturbed motion of a star induced by the presence of a companion.

## 1.3 Formation mechanisms of binary systems

The origin of binary stars is directly linked to that of single stars. The birth of a single star takes place in various stages:

- **Formation of a molecular cloud inside a galaxy.**
  The cloud is gravitationally bound and supported as a whole against the collapse by the presence of a magnetic field.
- **Formation of the molecular cloud cores.**
  Since the magnetic field tends to slowly leak out of over-dense regions of the

cloud via ambipolar diffusion, these ones are allowed to become more and more dense: in this way cores inside the molecular cloud are formed.

- **Collapse of the molecular cloud cores.**
  The cloud cores keep up increasing their density until their mass reaches a critical value called the Jeans mass $M_J$: as soon as $M > M_J$, they undergo the Jeans instability, which is a gravitational instability, and start to collapse towards stellar densities.

- **Formation of a central protostar embedded within an envelope of infalling gas and dust.**
  Each collapsing core originates a protostar, which is typically surrounded by a disk since the parental molecular cloud is almost always rotating; the newborn protostars accrete material from both the infalling cloud and the sorrounding disk, so that they grow embedded in a gas and dust envelope.

- **Development of protostars stellar winds.**
  As a protostar contracts towards the Zero Age Main Sequence (ZAMS), in order to become a star it develops a stellar wind directed to the system rotational poles; this is due to the fact that the infalling material deposits preferentially onto the disk, namely not onto the protostar surface, because of its high angular momentum.

- **Revelation of the protostars.**
  Since the ram pressure of the incoming material prevents the wind from breaking out, protostars remain unobservable for the large majority of their life; however, when the infall of material decreases, so that the opening angle of the wind widens, this one is able to escape, causing the expulsion of the protostellar disk: in this way, protostars become finally observable.

- **Formation of Pre-Main-Sequence (PMS) stars.**
  As soon as protostars become visible, they are considered PMS stars.

The PMS population is very rich in multiple systems: in fact, it has been estimated that the fraction of binaries exceeds the 50%, which means that binary formation can be assessed as the primary branch of the star formation process. In particular, since stars tendentially form in pairs, it is likely for binary formation to occur before the PMS stage.

As far as binary formation is concerned, three possible mechanisms have been proposed in order to explain it: tidal capture, prompt-fragmentation and delayed breakup (Tohline 2002).

### 1.3.1 Tidal capture

Tidal capture is a formation mechanism based on the fact that the cloud cores can collapse to form single stars which then become bound in pairs through tidal interactions arising from dynamical encounters.

In fact, the formation of a binary system from two initially unbound stars requires the dissipation of a fraction of their orbital energy: specifically, in favourable three-body encounters this energy can be transferred in form of kinetic energy to the perturbing star. Otherwise, binary systems can be the outcome of two-body encounters if the stars involved are close enough to make their interaction not only gravitational, but also tidal.

However, this scenario has been discarded for two main reasons: the former is related to the rarity of favourable three-body encounters, as in large virialised clusters the typical approach velocity of unpaired stars is hyperbolic, so that they tend to separate instead of becoming bound together, whereas the latter is due to the low probability of strong tides to be originated in two-body encounters unless the interacting stars are not very close. Therefore, in the absence of strong tides, too many encounters would be needed to dissipate a significant amount of energy and promote their approach.

### 1.3.2 Prompt-fragmentation

Prompt-fragmentation is a non-linear process characterised by the lack of simple symmetries and dependent on the type of collapse a molecular cloud undergoes. In fact there are two different mechanisms to be considered: the nearly homologous and the non-homologous collapse.

A rotating molecular cloud is defined to collapse in a nearly homologous fashion both if it has a spherical or spheroidal configuration and is uniform in density, and if its mass is significantly larger than the local Jeans mass (namely if $M \gg M_J^i$), whose value is the same almost everywhere inside the cloud. In this case the cloud evolves through a sequence of flatter and flatter configurations in a free-fall timescale determined by the mean local density $\overline{\rho} \simeq \overline{\rho}^i$. As the degree of flatness becomes more and more extreme, pressure gradients develop until they are able to slow down the collapse, so that the same final configuration is reached by all the cloud cores at approximately the same time.

On the other hand, a non-homologous collapse will occur if it starts from a centrally condensed or marginally Jeans unstable initial configuration inside the molecular cloud. In fact, the central regions of the cloud collapse ahead of the rest of it, so that

a steep density gradient is produced. This is due to the fact that, at every position inside the cloud, the collapse is governed by the local free-fall timescale, which differs according to the value of the mean local density: therefore, denser regions have shorter free-fall timescales and are likely to collapse first. At this stage either the cloud has a large enough angular momentum to stop the collapse, or the collapse continues and leads to the formation of an equilibrium core containing a small fraction of the cloud mass, followed by a period of mass accretion.

*N*-body simulations have shown that the nearly homologous collapse is probably the cause of prompt-fragmentation, whereas the non-homologous collapse seems to discourage it: in fact, the former mechanism favours the development and the amplification of non-axisymmetric density perturbations which can end up in the fragmentation of the cloud, whereas the latter retards the growth of such perturbations owing to the presence of strong pressure forces resulting from the steep density gradient it originates.
Nevertheless, it is not yet clear how often prompt-fragmentation will produce binary systems as the outcome of this process may be very sensitive to the spectrum of the initial density fluctuations. Hence a lot of work is still to be done in order to understand the relation between prompt-fragmentation and the formation of binary stars.

### 1.3.3 Delayed breakup

As already mentioned, the non-homologous collapse of a molecular cloud leads to the formation of a central equilibrium configuration, which can be referred to as a "core" and is stable against fragmentation; in addition to this, the core generally contains a small fraction of the cloud mass and may be enclosed in a rotationally supported accretion disk. Consequently, the evolution of the core will be driven in the first place by radiation losses and accretion, which cause both its mean density and its temperature to steadily rise; the same happens to the angular momentum, for accretion makes the core mass increase through the infalling of material either directly in from the cloud or migrating in from the sorrounding disk. The outcome of the combined processes is therefore a core which rotates faster and faster as contraction goes on. From now on the evolution of the core can be described by means of two theories, which are the classical view of fission and the Lebovitz's revised version of the fission theory.

According to the classical view of fission, the ellipsoid-shaped core will experience two possible figure deformations, becoming either pear-shaped or dumbbell-shaped: in the former case its progressive elongation due to rotation will make it end up in

two detached parts circularly moving around each other, so that a binary system will form. Since the fragmentation of the core takes place after it settles down to an equilibrium configuration, this formation mechanism is called delayed breakup. However, this scenario seems not to work because of both the instability of the pear-shaped configuration and the fact that the viscous timescale of protostars is too long for viscous dissipation to drive the evolution of the pear-shaped core. For this reason Lebovitz went through the classical fission theory and amended it in such a way that it could be independent from the action of viscosity.

Even so, none of these theories predicts that rapidly rotating axisymmetric cores can directly break up when they undergo the dynamical bar-mode instability which leads to their deformation: as a result, the delayed breakup mechanism has been rejected.

By way of conclusion, in spite of the fact that none of these scenarios is able to fully explain how binary systems originate from a parental molecular cloud, at the current time prompt-fragmentation is regarded as the most probable formation mechanism.

# Chapter II

# Fundamental parameters and distributions

A correct and complete physical description of binary systems is based on both the knowledge of eight fundamental parameters, which are the orbital elements and the mass of the components, and the derivation of three statistical distributions, i.e. the mass function,the mass-ratio distribution and the period distribution.

## 2.1 Orbital elements and mass of the components

In the study of binary systems two different problems have to be tackled: the former is of geometric type and consists in the determination of the orbital parameters, which allow a proper description of the relative orbit of both stars, and the latter has a purely astrophysical nature, since it deals with the estimate of some physical parameters, above which the mass of the components.
As far as the geometric problem is concerned, there are seven orbital elements which must be taken into account:

- The longitude of the ascending node $\Omega$.
- The inclination angle of the orbit plane $i$.
- The argument of the pericentre $\omega$.
- The semi-major axis of the orbit $a$.
- The eccentricity of the orbit $e$.

- The time of the passage at the periastron $T$.
- The revolution period $P$.

Besides, once the orbital elements are known the mass can be determined by combining Kepler's third law:

$$4\pi^2\frac{a^3}{P^2} = 4\pi^2\frac{(a_1+a_2)^3}{P^2} = G(M_1+M_2) \tag{2.1}$$

which can be written in a more compact form as:

$$\frac{a^3}{P^3} = M_1 + M_2 \tag{2.2}$$

with the relation:

$$\frac{M_2}{M_1} = \frac{a_1}{a_2} \tag{2.3}$$

## 2.2 Mass function

The mass function is used to constrain the mass of the unseen component of a binary system once the mass of the companion has been measured; therefore, it is defined for spectroscopic and photometric binaries.
The mass function is calculated from observable quantities only, such as the revolution period $P$, the eccentricity of the orbit $e$, the inclination angle of the orbit plane $i$, the semi-major axes $a_1$ and $a_2$ and the semi-amplitude $K$ of the radial velocity curve, which is obtained by plotting the observed radial velocities against the time.
However, the dependence of the mass function on these physical quantities varies from single-lined to double-lined spectroscopic binaries, as in the latter case both the stellar radial velocity curves are known, being one the opposite of the other.

For SBI the mass function can be written either as:

$$f(M_2) = \frac{M_2^3\sin^3 i}{(M_1+M_2)^2} = 1,035\times10^{-7}K_1^3P(1-e^2)^{\frac{3}{2}} \tag{2.4}$$

if the spectrum of the primary is observed, or as:

$$f(M_1) = \frac{M_1^3\sin^3 i}{(M_1+M_2)^2} = 1,035\times10^{-7}K_2^3P(1-e^2)^{\frac{3}{2}} \tag{2.5}$$

if that of the secondary is instead.
So, after the mass ratio:

$$\frac{M_2}{M_1} = \frac{a_1}{a_2} \tag{2.6}$$

has been evaluated through the gauge of $a_1$ and $a_2$, it is possible to provide an estimate of the mass.

On the other hand, by means of the reduced mass functions:

$$M_1 \sin^3 i = 1,035 \times 10^{-7} (K_1 + K_2)^2 P (1 - e^2)^{\frac{3}{2}} \tag{2.7}$$

$$M_2 \sin^3 i = 1,035 \times 10^{-7} (K_1 + K_2)^2 P (1 - e^2)^{\frac{3}{2}} \tag{2.8}$$

and if the inclination angle $i$ has been determined, for SBII the mass of the unseen component can be derived immediately from the mass ratio:

$$\frac{M_2}{M_1} = \frac{a_1}{a_2} = \frac{K_1}{K_2} \tag{2.9}$$

whose value descends directly from the analysis of the radial-velocity curves.

Since the mass function is strongly dependent on the mass of the primary $M_1$, it is occasionally helpful to work with this quantity instead:

$$Y = \frac{f(M_2)}{M_1} = \frac{q^3}{(1+q)^2} \sin^3 i \tag{2.10}$$

where:

$$q = \frac{M_2}{M_1} \tag{2.11}$$

is the mass ratio.
Hence the $Y$-distribution is a function of $Y$ defined as $\phi(Y)$.

Nonetheless, the $Y$-distribution may be affected by some selection effects because the mass function shows a heavy dependence also on $K$, especially in the case of single-lined spectroscopic binaries. In fact, small values of $K$, which come from either small inclinations or small mass ratios, are hard to detect: thus there may be a deficiency of small $K$ values, ending up in a $Y$-distribution peaked towards low values of $Y$.
Another selection effect, which actually yields the same result, is connected to stellar rotation. Since early-type stars rotate faster than late-type ones, their spectral lines are fuzzy and therefore small radial velocity variations may be overshadowed: as a consequence, if a large number of small radial velocity variations remains undetected,

a lack of small values of $K$ is expected. For this reason, the $Y$-distribution of early-type stars is more peaked towards small values of $Y$ than that of late-type ones.

## 2.3 Mass-ratio distribution

The mass ratio is defined as the ratio between the mass of the secondary and that of the primary of a binary system:

$$q = \frac{M_2}{M_1} \tag{2.12}$$

and represents one of the most relevant parameters for the characterisation of binary stars.
Its importance is related to the mass-ratio distribution, also called $q$-distribution, which not only displays the dependence of $f(q)$ on $q$, but is also regarded as a fundamental tool to investigate the dynamical processes binary systems went through during their life. In this sense, the $q$-distribution helps to build a bridge between binary physics and dynamics. Moreover, it provides an observational check for theoretical models of both binary evolution and star formation.

Many different shapes of the $q$-distribution have been proposed so far according to the sample of binaries examined and the initial conditions selected in $N$-body simulations, which are typically used to compare the observed $q$-distribution with the expected theoretical one.

As far as spectroscopic binaries are concerned, the $q$-distribution was found to be bimodal both by Hogeveen (1992), who analysed binary systems from *The Eight Catalogue of The Orbital Elements of Spectroscopic Binary Stars*, and by Trimble (1974), who based her work on *The Sixth Catalogue of Orbital Elements of Spectroscopic Binary Systems* instead.

According to Hogeveen, the $q$-distribution for the single-lined spectroscopic binaries in the sample has the form:

$$f(q) \propto q^{-\alpha} \begin{cases} \alpha=0 & \text{for } q<q_0 \\ \alpha=2 & \text{for } q>q_0 \end{cases} \tag{2.13}$$

where $q_0$ =0.3 for systems with B-type primaries and $q_0$ =0.55 for systems with K-type primaries. Hence, if $q<q_0$ the $q$-distribution is expected to be flat, whereas if $q>q_0$ it is a decreasing power-law.
On the other hand, the $q$-distribution for double-lined spectroscopic binaries has a

pronounced peak at $q \simeq 1$.
Thus the combination of the two distributions would yield a bimodal distribution with two maxima, the former placed at $q \simeq 0.25$ and the latter at $q \simeq 1$, if the selection effects affecting both single-lined and double-lined spectroscopic binaries were not carefully taken into account.
This is true in particular for SBII, as they are detectable only when the spectral lines of the secondary star are visible, i.e. if the primary is not much brighter than the secondary. What is more, the visibility of the secondary star spectral lines with respect to that of the primary ones can be expressed as a function of $q$:

$$g(q) = \frac{2}{1 + q^{-\beta}} \tag{2.14}$$

where typically $\beta \simeq 6$. Since $g(q)$ decreases rapidly with $q$, it follows that SBII with nearly identical components are harder to observe than those with different components: as a consequence, a selection effect does exist, for SBII with equally massive components are favoured. To cope with such a bias a large number of observations may be needed: therefore the determination the $q$-distribution could be a very difficult task.
For this reason, assuming for SBII the $q$-distribution assigned to SBI has been preferred in this case.

Trimble adopted a similar approach for the $q$-distribution setting, as she kept single-lined and double-lined spectroscopic binaries separated due to the presence of different selection effects. In fact, she found by analogy that the $q$-distribution of SBII peaks at $q \simeq 1$ because they are strongly concentrated towards high values of $q$. In particular, only few systems are characterised by mass ratios $q > 1$, which can be considered as an evidence of mass transfer being at work.
However, according to Trimble even SBI are affected by a selection effect, for their $q$-distribution peaks at $q \simeq 0.3$ but shows a sudden fall-off at very low values of $q$.
Since the SBII sample is biased in favour of high mass ratios, whereas the opposite happens for that of SBI, the two $q$-distributions have been combined together, so that an overall bimodal $q$-distribution has been obtained.

In the end, the $q$-distribution was found to be Gaussian-shaped by Kouwenhoven et al. (2009).

Hogeveen (1990) tried to constrain the shape of the $q$-distribution of visual binaries too by selecting a sample of binary systems from both *The Fourth Catalogue Of Orbits Of Visual Binary Stars* and the revised version of *The Index Catalogue Of Visual Double Stars*. He found that the most important selection effects at stake were:

- The maximum and minimum orbital separation between the components, as

limits for the detection of the binaries.

- The maximum apparent magnitude of the primary, since too faint primaries must be rejected in order to make a sound statistics.
- The maximum apparent magnitude difference between the components because, if either the primary is too bright or the secondary too faint, the latter may be undetected, so that the system will not be recognised as double.

By taking these selection effects into consideration and resorting to simulations, Hogeveen concluded that the observed $q$-distribution was in agreement with the real one for $q>0.25$ and could be reproduced by the power-law:

$$f(q) \propto q^{-2.7} \tag{2.15}$$

whereas for $q<0.25$ this did not occur owing to the selection effects predominance. For this reason, the $q$-distribution was assumed to be flat in the range $0<q<0.25$, thus obtaining the following result:

$$f(q) \propto q^{-\alpha} \begin{cases} \alpha=0 & \text{for } q<0.25 \\ \alpha=2.7 & \text{for } q>0.25 \end{cases} \tag{2.16}$$

From the knowledge of the $q$-distribution, also the companion mass-ratio distribution (CMRD), which displays the trend of the mass ratio $q$ as a function of the primary mass $M_1$, can be calculated.
In the work by Reggiani, M. and Meyer, M. R. (2013) it has been argued that, unlike the $q$-distribution, the CMRD appears to be universal over a wide range of $q$ values and primary masses, as it can be described by the power-law:

$$f(q) \propto q^{-\beta} \tag{2.17}$$

where the best-fit value of the exponent seems to be $\beta=0.25\pm0.29$, as derived from the combination of the $q$-distribution for M-dwarfs and that for solar-type stars.

Furthermore, the shape of the CMRD is unaffected by dynamics, for binaries with high $q$ values are destroyed as well as those having low $q$ values, without any preference. In fact, the survivability of a binary system shows a weak dependence on the mass ratio because the binding energy:

$$E_{bind} = -\frac{G(M_1 M_2)}{2a} \tag{2.18}$$

is proportional to the mass of both the primary and the secondary component.

Since binary stars are typically destroyed in dynamical interactions with perturbing single stars, another important quantity to take into account is the kinetic energy of these ones:

$$E_{K,p} = \frac{1}{2} M_p v_p^2 \tag{2.19}$$

Thus the fate of binary stars is determined by the value of their binding energy: if the binding energy is lower than the kinetic energy of the perturbing stars, then binary systems will be disrupted; the opposite happens when the binding energy is greater than the kinetic energy of the perturbing stars. Hence, from a dynamical point of view binaries can be either soft or hard.
In particular, by means of *N*-body simulations Parker and Reggiani (2013) demonstrated that, for a binary system to be broken up during an interaction, the kinetic energy of the perturbing star must exceed the binding energy of the system by a factor from 10 to 100, i.e. $E_{K,p} \simeq$ 10-100 $E_{bind}$, which means that the dependence of $E_{bind}$ on $q$ is negligible. Consequently, the harder the binary, the higher the ratio $\frac{E_{K,p}}{E_{bind}}$.

This result has raised considerable interest: if the CMRD is not affected by dynamical evolution, then it may be employed as a strong diagnostic of the universality of the star formation process. In fact, changes in the shape of the observed CMRD may be attributed to the variability of the binary systems physical properties according to the environment in which they have formed. Therefore, the CMRD of different star forming regions can indicate the presence of separate modes of star formation.

## 2.4 Period distribution

The period distribution is another useful instrument to investigate the dynamical processes affecting binary evolution. In fact, the period $P$ is directly linked to the orbital separation $a$ between the components of a binary system: large values of $a$ imply long periods (wide binaries), whereas small values of $a$ entail shorts periods (tight binaries).

According to Korntreff, Kaczmarek, and Pfalzner (2012), the observed log-normal period distribution for a field binary population made of both G-type stars and M-dwarfs in the solar neighbourhood is different from the primordial one, which is supposed to be log-uniform, because of binary dynamical evolution. In fact, there are two main processes acting in changing the period distribution:

- **Gas-induced orbital decay.**
  Since star formation takes place in gas clouds, the newborn stars go through

an embedded phase before the gas is completely removed by the strong winds originated by both very massive stars, i.e. OB stars, and supernova explosions. In particular, binary systems experience the dynamical friction with the sorrounding gas during this phase, so that they lose energy and momentum: as a result, the orbital separation between the components decreases and their merging in favoured. Thus, gas-induced orbital decay diminishes the fraction of short-period binaries, for they are characterised by small orbital separations.

- **Dynamical destruction in three- or four-body encounters.**
  Wide binaries are typically destroyed in encounters because their binding energy is lower then the kinetic energy of the perturbing stars: therefore, when part of this kinetic energy is transferred to the binary components, they tend to depart from each other, causing the dissolution of the systems they belong to. For this reason, three- or four-body encounters reduce the fraction of long-period binaries.

What is more, the two processes never act together as they affect different periods; in fact, since the maximum period for gas-induced orbital decay is $P_{orb,max} \simeq 5.5 \times 10^4$ days and that for three- or four-body encounters is $P_{dyn,max} \simeq 1.1 \times 10^5$ days, it follows that $P_{orb} < P_{dyn}$.

In conclusion, these dynamical processes do change the distribution of binary stars periods, so that their combined effect leads to the transformation of the primordial log-uniform period distribution into the log-normal period distribution observed at the present time.

# Chapter III

# Binary stars and stellar dynamics

## 3.1 Star clusters as collisional systems

Star clusters constitute great "laboratories" to investigate stellar dynamics; since gravity (for which the Newtonian approximation holds) is generally the predominant force in stellar systems, any star cluster can be regarded as a self-gravitating "gas" of stars and therefore treated as a fluid. Consequently, fluid dynamical models are suitable for the theoretical description of stellar systems.
In the fluid dynamical approach, a stellar system is fully represented by an evolving phase-space and seven-variable-dependent density distribution $f(\vec{r},\vec{v},t)$, which the following boundary conditions are associated to:

$$f \longrightarrow 0 \text{ if } r, v \longrightarrow \pm\infty \tag{3.1}$$

for the system is finite and $f(\vec{r},\vec{v},t)\geq 0$. The evolution of $f(\vec{r},\vec{v},t)$ is determined through the Fokker-Planck equation, as it accounts for dynamical processes related to two-body relaxation which the Boltzmann equation, outlining collisionless systems, does not include.
On the other hand, the velocity distribution $f(\vec{v},t)$ is assumed to be a Maxwellian.

Star clusters are defined as collisional systems because two-body encounters are the main drivers of their dynamical evolution; in particular, encounters can be either strong or weak.
Strong encounters produce large energy variations as they imply the fly-by of two different stars; in fact, when a star passes very close to another one, there will be not only a modification of the perturbed star orbit, but also a variation of its velocity of the order $\Delta v \sim v$.

Besides, the typical timescale for strong encounters is given by:

$$t_s \approx 4 \times 10^{12} \left( \frac{v}{10 kms^{-1}} \right)^3 \left( \frac{M}{M_\odot} \right)^{-2} \left( \frac{n}{1 pc^3} \right) \text{ yr} \tag{3.2}$$

where $v \sim 10$ km s$^{-1}$ and $n \geq 1000$ pc$^{-3}$ for globular clusters. Thus, since $t_s$ is important for small stellar velocities, it is clear that strong encounters are common in GCs (i.e. one or even more strong encounters per star).

Instead, weak encounters are not responsible for a significant alteration of the stellar energy balance for they do not consist in the real approach of different stars, but are due to long-distance interactions: in fact, each weak encounter causes the other stars path to be deflected only by a small angle, which means that on the whole the orbits will remain unperturbed.
However, stars in clusters normally undergo many weak encounters during their life, so that there is a cumulative effect: hence the total deflection angle will be large. Furthermore, weak encounters act in a selective way on stellar velocities, as they affect only the velocity component perpendicular to the line of sight.

## 3.2 Relaxation and its consequences

Relaxation is the response of a system to a perturbation: in fact, it consists in the return of a perturbed system to an equilibrium state. The concept of relaxation is connected to the so called relaxation time, which is a measure of the time it takes for an object to be significantly perturbed by another one inside a system. Nevertheless, relaxation time is most commonly defined as the time for a star either to lose all memory of its initial orbit or to experience a velocity variation of order itself because of encounters:

$$t_{relax} = \frac{t_s}{2 \ln \left( \frac{b_{max}}{b_{min}} \right)} \tag{3.3}$$

where $b$ is the impact parameter. In particular, $t_{relax}$ depends on the integration limits, for $b_{max}$ is the characteristic size of the whole stellar system and $b_{min}$ is assumed to be the strong encounter radius:

$$r_s = \frac{2GM}{v^2} \tag{3.4}$$

Since $t_{relax} \sim 100$ Myr for both globular and open clusters, it follows that relaxation time is shorter than the lifetime of globular clusters, but is comparable to that of open

clusters: therefore, the importance of this result lies in its pointing out the impact of encounters in the evolution of stellar systems.

Regarding cluster dynamics, relaxation has some crucial consequences (Spitzer 1987):

- **Evaporation.**
  Since two-body relaxation allows stars to exchange energy among themselves, they will become unbound and therefore leave the cluster if their total energy ends up to be greater then the cluster escape velocity; moreover, tidal shocks can accelerate the escaping process by implanting additional kinetic energy to them. In particular, tidal shocks are originated by the passage of stars close either to the Galactic centre in the case of GCs, or to giant molecular clouds and spiral density waves in that of OCs.
  However, evaporation can be enhanced by stellar evolution too because high-mass stars typically die before the low-mass ones: in this way each cluster loses part of the high-mass stars it had at birth.
  In the end, it is worth stressing the role of binaries with respect to evaporation. As binaries have more kinetic energy than single stars, simply because they are made of two components moving around each other instead of one, they tend to make space and to occupy a bigger volume: consequently, stars in the outskirts are pushed further out, which facilitates their being lost by the system.

- **Mass segregation.**
  Mass segregation consists in the progressive sinking of high-mass stars towards the centre of a cluster; it is due to the fact that two-body relaxation seeks to equalise the kinetic energy of different mass stars, so that the more massive ones are forced to move to the inner regions because of their smaller velocities.

- **Core collapse.**
  Just as mass segregation, core collapse is triggered by the two-body relaxation attempt of compensating the kinetic energy of different mass stars; in fact, stars in the cluster cores are characterised by high velocities, so that they lose energy when trying to equalise the kinetic energy of those in the outskirts: for this reason they sink even further towards the centre. Hence core collapse can be dramatically accelerated by mass segregation depending on the energy of the individual stars.
  In particular, binary stars play a big part in preventing core collapse from happening through the injection of energy, for they tend to increase the velocity of the system they belong to.

Thus evaporation, mass segregation and core collapse, together with stellar evolution,

are the dynamical processes which determine the evolution of star clusters, as they are responsible for the reshuffle of their native stellar configuration. On the other hand, the post-collapse evolution of such systems is related to their initial conditions: if a system is isolated, then it will experience the binary induced mass loss, whereas if it is tidally limited, it will lose mass because stars crossing the tidal radius, beyond which external forces become important, are fated to escape.
When a stellar system undergoes one or more of these processes, it is defined to be out of virial equilibrium, i.e. it does not satisfy the virial equation:

$$2E_K + E_P = 0 \tag{3.5}$$

where $E_K$ is the kinetic energy and $E_P$ the potential energy of the system.

## 3.3 The King model for globular clusters

Globular clusters represent an interesting class of stellar systems for their structure and original stellar distribution are significantly altered because of the dynamical processes previously discussed.
A proper description of globular clusters evolution is therefore given by the King model, whose functional form is:

$$f = k\left(\frac{1}{\sqrt{1+\left(\frac{r}{r_c}\right)^2}} - \frac{1}{\sqrt{1+\left(\frac{r_t}{r_c}\right)^2}}\right)^2 \tag{3.6}$$

where $r_c$ is the core radius, i.e. the radius at which the superficial brightness becomes half of its central value, whereas $r_t$ is the tidal radius, which marks the borders of these systems.
The King profile is flat in the regions going from the centre to the core radius and decreases outside it (Fig. 3.1, left panel).

In particular, the King model is characterised by the so called concentration parameter:

$$c = \log\left(\frac{r_t}{r_c}\right) \tag{3.7}$$

which indicates how much mass is concentrated towards the centre of a globular cluster.
As a consequence, different values of $c$ are connected to different dynamical stata: the

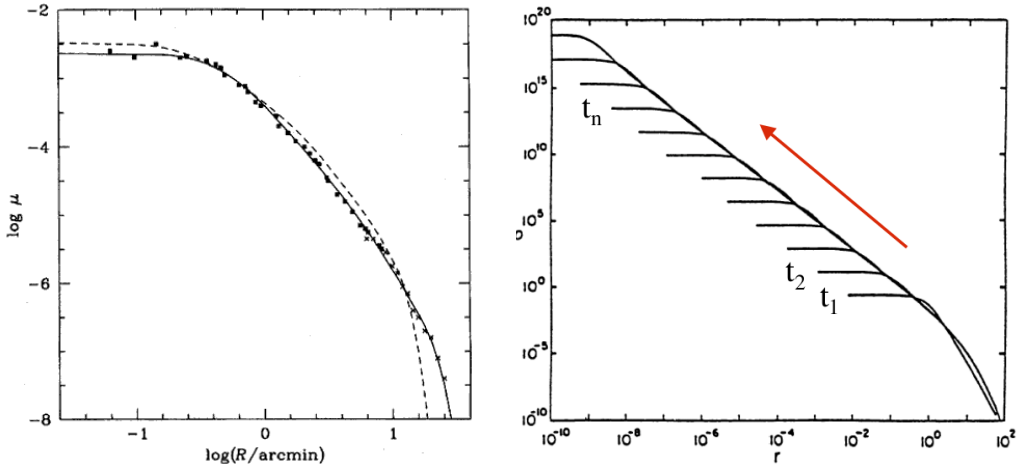


Figure 3.1: Left panel: King profile. Right panel: Modified King profile.

higher the concentration parameter, the more evolved the stellar system. In this sense, King models at varying $c$ provide an overview about the dynamics of globular clusters.

However, King models, despite being quasi-stationary, become gravothermally unstable above a certain concentration: this occurs in the case of globular clusters experiencing core collapse. Such an instability manifests itself ciclically and is triggered by the shrinking of the core, which makes not only the potential energy, but also the temperature rise. Consequently, the kinetic energy increases too, producing two different effects, i.e. the balance with the potential energy and the departure of faster stars, which favours a further shrinking of the core.
The only way to stop the collapse is to provide a source of energy in the centre, especially through the presence of binaries, in order to replace the escaped heat.

Therefore, since the gravothermal instability is responsible for the progressive increase of the concentration parameter, the King model cannot be described by a flat profile in the inner regions of globular clusters anymore: a power-law cusp appears to be suitable instead (Fig. 3.1, right panel).

## 3.4 Binary population in star clusters and in the field

Even if most stars in the field are observed in multiple systems, binarity is far more common in young star clusters, for at least 50% of stars probably form in such environments. However, internal dynamical processes, depending on both the density and the lifetime of the cluster, may not only significantly affect the properties of the

hosted binary population, but also rapidly change the binary fraction. For this reason, the binary field population is likely to be composed of binaries dynamically processed in various ways as coming from different density environments.

In order to determine whether binaries in clusters form in the same way as in the field or not, Parker et al. (2009) investigated the evolution of a field-like binary population in star clusters by means of *N*-body simulations; as such, this analysis enabled the calculation of the number of processed binaries in accordance with the orbital separation $a$ between their components.
Since the binary population in different density clusters is related to the position of the so called hard-soft boundary:

$$a_{h-s} \propto \frac{r_{\frac{1}{2}}}{N_b} \tag{3.8}$$

where $r_{\frac{1}{2}}$ is the half-mass radius of the cluster and $N_b$ the number of binary stars, dense clusters, i.e. globular clusters, characterised by $\rho\sim$ $10^4$-$10^5$ $M_\odot$ $pc^{-3}$, have been examined separately from low-density clusters, i.e. open clusters, which typically have $\rho\sim$ $10^2$ $M_\odot$ $pc^{-3}$ instead.

Since the hard-soft boundary is placed at a few hundred AU in globular clusters, both sometimes-hard binaries ($a\sim$50-1000 AU) and soft-intermediate binaries ($a\sim$ $10^3$-$10^4$ AU) are mostly destroyed, whereas always-hard binaries ($a\leq$50 AU) are not; on the contrary, always-soft binaries ($a\geq$ $10^4$ AU) are completely disrupted during the first $\sim$0.1 Myrs of the cluster lifetime, which is nearly a crossing time.
As a consequence, this result suggests that after $\sim$0.1 Myr globular clusters are able to reach an equilibrium which assures the binary fraction to remain roughly constant: therefore, the binary population in dense environments should be processed and set in its final configuration in a very short timescale.
On the other hand, in open clusters the hard-soft boundary is shifted towards lower values with respect to globular clusters, so that not only always-hard, but also sometimes-hard binaries are not destroyed; nevertheless, such a shift is not big enough to prevent the disruption of some soft-intermediate and of all always-soft binaries.

Thus there are three important conclusions to be drawn:

- The binary fraction at $a<$50 AU must be a direct outcome of the star formation process, because always-soft binaries are never destroyed, independently of the density of their parental environment: therefore, only for such separations binaries in clusters form with a field-like distribution.
- Cluster dynamics does not allow always-soft binaries to survive or even to form for they are too loosely bound, although very wide binary systems exist in the

field.

- Since the binary fraction in dense clusters is very similar to that of the field, whereas in sparse clusters it is higher, it follows that binaries are much more affected by stellar dynamics in globular than in open clusters. In fact, binaries in star clusters are altered by gravitational interactions, i.e. three- or four-body encounters, and tend to become either softer if soft or harder if hard according to the Heggie-Hills law.

As proposed by Kaczmarek, Olczak, and Pfalzner (2011), to better understand the properties of the presently observed binary population, the primordial binary population must be assessed, i.e. the binary population as it appears just after the end of the star formation process: therefore, young dense star clusters are the ideal environments for this purpose.
Still, since the binary fraction:

$$f_b(t) = \frac{N_b(t)}{N(t)} = \frac{N_b(t)}{N_s(t) + N_b(t)} \tag{3.9}$$

where $N_b(t)$ is the number of binary systems and $N_s(t)$ that of single stars is a function of time, can be biased due to its dependence on $N_s(t)$, a more reliable quantity to take into account for investigating the evolution of the binary population is the normalised binary fraction:

$$f_{b,norm}(t) = \frac{N_b(t)}{N_b(0)} \tag{3.10}$$

where $N_b(0)$ is the initial number of binaries.
Despite both $f_{b,norm}$(t) and $f_b(t)$ decrease in time because of the preferred destruction of wide binaries in encounters, the former does not depend on the initial binary fraction $f_b(0)$, whereas the latter does: this can be explained by considering that single star evolution has a non-negligible impact on binary evolution, for $N_s(t)$ increases over time as a result of the dissolution of wide binaries. Hence, the higher the number of primordial wide binaries, i.e. the primordial binary fraction $f_b(0)$, the higher also the number of single stars $N_s(t)$ originated from binary evolution, i.e. the lower the binary fraction $f_b(t)$.
In particular, $f_b(0)$ can be expressed by means not only of $f_b(t)$, but also of an evolving function $\alpha(t,f_b(t),...)\approx\alpha(t)$ such that $N_b(t)= \alpha N_b(0)$:

$$f_b(0) = \frac{f_b(t) - \alpha(t) + 1}{\alpha(t)} \tag{3.11}$$

If the exact form of $\alpha(t)$ can be determined and $f_b(t)$ is known, then this equation

immediately yields $f_b(0)$: for instance, in this way it has been estimated that $f_b(0)\approx 74\%$ in the Orion Nebula cluster (Kaczmarek, Olczak, and Pfalzner 2011).

Furthermore, the binary population in young dense star clusters is influenced also by the value of the primary mass, as observations point out that massive stars, i.e. stars with $M>2$ $M_\odot$, are more commonly found in binary systems than low-mass ones.
In fact, the binary fraction of low-mass-primary systems $f_{b,low}(t)$ changes very rapidly for two main reasons:

- Binaries with low-mass primaries are typically destroyed in three-body encounters because of the lower binding energy.
- The possible generation of a high-mass and a low-mass star in the dissolution of binary systems with massive primaries accelerates the reduction of $f_{b,low}(t)$, but decelerates that of $f_{b,high}(t)$. In fact, if binaries having different mass components are disrupted, then the number of single low-mass stars tends to steadily increase, so that $f_{b,low}(t)$ decreases, whereas that of single high-mass stars does not: by implication, the binary fraction of high-mass primaries $f_{b,high}(t)$ barely rises.

So, on a final note, the difference between $f_{b,low}(t)$ and $f_{b,high}(t)$ appears to be linked to cluster dynamical evolution, since the lower the primary mass, the more likely for a binary system to be subjected to dissolution.

## 3.5 How do binaries affect the total star cluster mass?

The total mass of a stellar system, such as a star cluster, can be determined in two different ways:

- By using the $\frac{M}{L}$ ratio taken from a single-stellar-population model in order to convert beyond the age, derived by the knowledge of the metallicity and the IMF, both the observed luminosity and distance directly into mass. Thus this method is based on star counts and yields the so called photometric mass $M_{phot}$.
- Through the virial theorem, which returns the dynamical mass:

$$M_{dyn} = \eta \frac{r_{\frac{1}{2}} \sigma_{los}^2}{G} \tag{3.12}$$

  where $r_{\frac{1}{2}}$ is the half-mass radius of the cluster, $\sigma_{los}$ the line-of-sight velocity dispersion and $\eta$=9.75 a dimensionless proportionality constant.
  In particular, this expression for $M_{dyn}$ relies on the following assumptions:

- The cluster dynamics can be described by means of the Plummer model.
- The cluster is in virial equilibrium.
- All the stars in the cluster are single and of equal mass.
- No selection effects are present.

An inconsistency between the two mass estimates for the same star cluster is attributed either to a lack of virial equilibrium or to the presence of a considerable number of unresolved binaries.
In fact, according to Gieles, Sana, and Portegies Zwart (2010), if on the one hand $M_{phot} \approx M_{dyn}$ for clusters older than 100 Myr, on the other $M_{dyn} > M_{phot}$ for young star clusters ($\sim$10 Myr) because $\sigma$ is very high. Such systems may be in a super-virial state due the violent expulsion of residual gas from the parental molecular cloud via stellar winds or supernova explosions: as a consequence, the newborn stars should experience a significant velocity increase with respect to their binding energy. However, the gas-expulsion scenario is not completely compatible with the onset of a super-virial state, as the estimated densities for young star clusters seem to be too high to make any feature of gas expulsion detectable in the measured velocity dispersion. Therefore, this theory has been discarded in favour of another one, which accounts for the effects of unresolved binaries in star clusters.

Since an overestimation of $M_{dyn}$ is typical of young stellar systems, whose light is dominated by massive stars ($M \geq 15$ $M_\odot$ at birth), for which binarity is high, it follows that an enhancement in the observed velocity dispersion is most probably related to binaries. In fact, massive binaries have a major impact on $\sigma$ than low-mass ones not only because of their higher orbital velocities, but also for their shorter orbital periods. As highlighted by Kouwenhoven and de Grijs (2009), binary systems tend to inflate $\sigma_{los}$ for their components move both in the cluster gravitational potential (particle motion) and in the binary itself (orbital motion); consequently, the binary line-of-sight velocity dispersion $\sigma_{los,b}$ is given by the superposition of two different contributions:

$$\sigma_{los,b} = \sigma_{part} + \sigma_{orb} \tag{3.13}$$

In particular, $\sigma_{orb}$ is much more important at increasing binary fraction, so that in binary-dominated clusters, such as open clusters, $\sigma_{los,b} \approx \sigma_{orb}$; typically $\sigma_{los,b} \leq 1$ Km s$^{-1}$ in this case.
Nevertheless, there are other parameters affecting the value of $\sigma_{orb}$ besides the binary fraction:

- **Period distribution *f(P)*.**

Since:

$$\sigma_{orb} \propto \sqrt{P} \tag{3.14}$$

clusters containing a large number of wide binaries exhibit a lower value of $\sigma_{orb}$ owing to their longer orbital periods.

- **Eccentricity distribution *f(e)*.**
  Stars in eccentric orbits generally spend most of their time near the apastron and have therefore small orbital velocities: by implication, clusters hosting many binaries with eccentric orbits are expected to have a lower $\sigma_{orb}$.

- **Mass ratio $q$.**
  When a binary system is composed by different mass stars, i.e. by a massive primary and a low-mass secondary in most cases, then the value of $\sigma_{orb}$ changes according to which star is detected. Since the most massive component is generally measured due to its major brightness, the result is that binaries with small mass ratios will give a small contribution to $\sigma_{orb}$.

On the contrary, $\sigma_{orb}$ doesn't depend on the value of the half-mass radius $r_{\frac{1}{2}}$, i.e. on the size of the cluster, like $\sigma_{part}$ because:

$$\sigma_{part} \propto \frac{1}{\sqrt{r_{\frac{1}{2}}}} \tag{3.15}$$

Hence the bigger the cluster, the smaller $\sigma_{part}$. This can be explained by considering that large clusters are also very dense, so that stars are forced to move more slowly in the cluster potential.

So, the kinematic bias introduced by binaries appears to be relevant only where the binary fraction is high, namely in open clusters.
In fact, even if unresolved binaries can alter the proper-motion dispersion profiles of globular clusters (Bianchini et al. 2016), their effect is mitigated by the presence of a limited number of binary stars in such systems.

On the other hand, when the cluster mass is evaluated through the luminosity function (LF) obtained via star counts, i.e. as photometric mass $M_{phot}$, the mass estimate derived by neglecting unresolved binaries will result smaller than the actual mass.
In fact, if a single star and a binary system share the same magnitude, then also their luminosities are equal:

$$L_s = L_1 + L_2 \tag{3.16}$$

where the suffix $s$ marks the single star, while *1* and *2* the primary and the secondary

respectively. So, given the relation:

$$\left(\frac{L}{L_\odot}\right) \sim \left(\frac{M}{M_\odot}\right)^4 \tag{3.17}$$

which is valid for MS stars, it follows that $M_s^4 < (M_1 + M_2)^4$ because:

$$M_s^4 = M_1^4 + M_2^4 \tag{3.18}$$

whereas:

$$(M_1 + M_2)^4 = M_s^4 + 4M_1M_2^3 + 6M_1^2M_2^2 + 4M_2^3 \tag{3.19}$$

Consequently, being all the terms positive, it can be concluded that:

$$M_s^4 < (M_1 + M_2)^4 \Longrightarrow M_s < M_1 + M_2 \tag{3.20}$$

In order for the photometric mass to become a reliable estimate of the total cluster mass, a multiplicative correction factor is needed.
For instance, according to Khalaj and Baumgardt (2013), who took account of the presence of unresolved binaries in Preasepe, such a correction factor attains the value of 1.35. However, since little information was provided about the methods of its estimation, further analyses have been made by Borodina et al. (2019), who investigated the effects of unresolved binaries in the derivation of the mass of five open clusters, i.e. IC 2714, NGC 1912, NGC 2099, NGC 6834 and NGC 7142, by star counts.
Owed to the dependence of the correction factor on both the binary fraction and the mass-ratio distribution, a stellar-magnitude-independent binary fraction has been adopted and different realistic $q$-distributions have been considered (i.e. a Gaussian distribution with either $\mu_q$=0.23 or $\mu_q$=0.60 and a flat distribution), so that several models have been realised.
In particular, it has been found that the increment value for the photometric mass ranges between 1.10 and 1.15, although it may increase up to 1.32 if not only binaries, but also multiple systems, are included: thus, in this case the value of 1.35 proposed by Khalaj and Baumgardt seems to be reasonable.

# Chapter IV

# *N*-body simulations

## 4.1 The *N*-body problem

*N*-body simulations are born to study both the physics and the dynamical evolution of self-gravitating systems by applying Newton's law of gravity to the *N* bodies these ones are composed of (Aarseth 2010). The basement of *N*-body simulations is the so called *N*-body problem, defined by the set of second-order differential equations:

$$\ddot{\vec{r}}_i = -G \sum_{j=1, j\neq i}^{N} \frac{M_j(\vec{r}_i - \vec{r}_j)}{\left|\vec{r}_i - \vec{r}_j\right|^3} \tag{4.1}$$

which indicate the force per unit mass $\vec{F}_i$ exerted by a particle of index $j$ on another one of index $i$ in a system of $N$ particles. If the initial conditions $M_{i,in}$, $\vec{r}_{i,in}$, $\vec{v}_{i,in}$ for the mass, the position and the velocity of each particle at some instant $t_0$ are added to the system, then it will be formed by $3N$ second-order differential equations, whose solutions $\vec{r}_i$ exist in the time interval $(-\infty,+\infty)$.
Otherwise, the complete solutions of such system can be found by replacing the $3N$ second-order differential equations above with $6N$ first-order differential equations to be solved in a self-consistent manner.
However, it is a matter of fact that the *N*-body problem thus introduced admits exact solutions only in the case of two interacting particles.

## 4.2 *N*-body tools

*N*-body simulations make use of several tools and algorithms both to obtain a proper description of the processes affecting self-gravitating systems and to reduce and speed up as much as possible computer calculations. The most important ones are force polynomials, individual and block time-steps, Hermite integration, neighbour treatments and regularisation procedures.

### 4.2.1 Force polynomials

Since the force $\vec{F}$ acting on a particle of a *N*-body system can be considered as smoothly-varying on some timescale throughout the orbit, it is reasonably approximated by a continuous function. Thus, given the values of $\vec{F}$ at four successive past times $t_3$, $t_2$, $t_1$, $t_0$, where $t_0$ is the most recent one, $\vec{F}$ can be written in the form of a fourth-order fitting polynomial at a time t$\in$[$t_3$, $t_o$+$\Delta t$] by using the divided difference formulation:

$$F_t = (([D^4(t-t_3) + D^3](t-t_2) + D^2)(t-t_1) + D^1)(t-t_0) + F_0 \tag{4.2}$$

where:

$$D^k[t_0, t_k] = \frac{D^{k-1}[t_0, t_{k-1}] - D^{k-1}[t_1, t_k]}{t_0 - t_k} \tag{4.3}$$

for $k$=1,2,3 is exactly the divided difference.
Force polynomials are not only essential to deal with the force summation, but also facilitate the prediction of coordinates.

### 4.2.2 Individual and block time-steps

In *N*-body simulations each particle is typically assigned its own individual time-step:

$$\Delta t_i = \sqrt{\frac{\eta \left|\vec{F}\right|}{\left|\vec{F^{(2)}}\right|}} \tag{4.4}$$

where $\eta$ is a dimensionless constant, as real stellar systems are characterised by a range in density which gives rise to different timescales associated to non-negligible changes of the orbital parameters; for this reason, time-steps are chosen according to the orbital timescales.

In particular, if two different mass particles are involved in a strong interaction, then their time-steps will be very similar, which has some practical advantages in view of minimising computer calculations.
It is also possible to quantise time-steps in blocks though, so that a group of particles can be analised and therefore advanced at the same time in the integration.

### 4.2.3 Hermite integration

The divided difference formulation of the force polynomials has been recently replaced by the Hermite integration, which grants not only a simpler handling of their computational evaluation, but also more accurate results. Moreover, since the Hermite scheme employs a Taylor series to express both the force $\vec{F}$ and its first derivative $\vec{F}^{(1)}$ and adds the high-order derivatives $\vec{F}^{(2)}$, $\vec{F}^{(3)}$ as correctors, it has the effect of speeding up calculations.

### 4.2.4 Neighbour treatments: the Ahmad-Cohen method

$N$-body simulations may frequently become very time-consuming due to the large star clusters memberships: therefore neighbour treatments have been introduced in order to reduce computational timings. In particular, the Ahmad-Cohen method has proved very effective in this sense, for it aims to minimise the effort of evaluating the force contribution from distant particles by combining two polynomials related to different timescales.
This is done by splitting the total force acting on a given particle into a regular and an irregular component:

$$\vec{F} = \vec{F}_R + \vec{F}_I \tag{4.5}$$

thus obtaining two force polynomials, so that the summation over the full particles number $N$ can be replaced by a sum over the $n$ nearest particles, which are labelled as neighbours, together with a prediction of the distant contribution.
The Ahmad-Cohen method has been implemented by means of the Hermite integration to provide appropriate corrections to both the force polynomials anytime a change of neighbour occurs, i.e. in binary interactions: as a consequence, it appears to be suitable especially for regularisation procedures.

### 4.2.5 Two-body regularisation

The presence of binaries and multiple systems in star clusters must be treated by using specific techniques to obtain satisfactory results in $N$-body simulations. During the integration of a $N$-body system, close encounters generate configurations that are difficult to handle with direct methods, i.e. binaries characterised by large eccentricity values, thus requiring small time-steps in the pericentre region in order to be properly studied. For this purpose regularisation procedures have been implemented.

Since primordial binaries are a fundamental ingredient of realistic star cluster simulations, two-body regularisation has been carefully developed.
The perturbed two-body problem, which two-body regularisation is based on, is given by the second-order differential equation:

$$\ddot{\vec{R}} = -\frac{(M_i + M_j)}{R^3 + \vec{F}_{ij}}\vec{R} \tag{4.6}$$

describing the relative motion of a binary with mass components $M_i$ and $M_j$ under the action of the external perturbation $\vec{F}_{ij}$=$\vec{F}_i$-$\vec{F}_j$.
The essential idea of two-body regularisation is to transform both the time and the coordinates associated to a binary system by means of the Kustaanheimo-Stiefel (KS) method; therefore the differential time transformation, connecting physical and regularised time, is given by:

$$dt = R^n d\tau \tag{4.7}$$

where $n$ is an arbitrary exponent, whereas the transformed coordinates are:

$$\vec{R}_1 = u_1^2 - u_2^2 \quad , \quad \vec{R}_2 = 2\vec{u}_1\vec{u}_2 \tag{4.8}$$

and satisfy the relations:

$$R = u^2 = u_1^2 + u_2^2 + u_3^2 + u_4^2 \quad , \quad \vec{R} = L(\vec{u})\vec{u} \tag{4.9}$$

where L($\vec{u}$) is the Levi-Civita matrix:

$$L(\vec{u}) = \begin{pmatrix} u_1 & -u_2 & -u_3 & u_4 \\ u_2 & u_1 & -u_4 & -u_3 \\ u_3 & u_4 & u_1 & u_2 \\ u_4 & -u_3 & u_2 & -u_1 \end{pmatrix} \tag{4.10}$$

Then, the centre of mass is introduced as a fictitious particle described by its appropriate

force polynomial: as a consequence, a complete description of two-body motion is obtained by integrating the centre of mass as a single particle together with the relative motion for each KS pair.
Moreover, assuming that the two-body orbit is conserved over one or more periods, the KS method allows to treat binaries as single stars, so that integration becomes easier.

To conclude, two-body regularisation has been recently improved by the adoption of the Stumpff-Hermite formulation, which is based on the so called Stumpff functions; such procedure includes correction terms for higher orders of integration whereby small perturbations need to be taken into account, thus ensuring a significant upgrade of KS solutions.

### 4.2.6 Multiple regularisation

From observations of both the solar neighbourhood and Galactic star clusters it appears evident that triples, as well as high-order systems, are very common.
The main formation channel of triples is given by binary-binary collisions according to the scheme:

$$B + B \Longrightarrow [B, S] + S \tag{4.11}$$

where $B$ indicates a binary, whereas $S$ a single star; multiple encounters are likely to be responsible for the creation of high-order systems instead. Therefore, the presence of binaries, especially hard ones, inevitably leads to close encounters which imply large energy variations.
Since the KS method may be insufficient to deal with such strong interactions in $N$-body simulations, multiple regularisation has been implemented: it is usually distinguished into three-body regularisation, which is applied to triples, and chain regularisation, which is suitable for quadruples and high-order systems instead.

Three-body regularisation consists in the introduction of two coupled KS regularisations based on the time transformation:

$$dt = \vec{R}_1 \vec{R}_2 d\tau \tag{4.12}$$

and on the coordinate transformation:

$$Q_k^2 = R_k \tag{4.13}$$

for $k$=1,2, from the binary components to the third body.
The new coordinates allow to write the equations of motion for the three-body problem

in such a way that a practical regularisation can be achieved.

On the other hand, chain regularisation begins with the introduction of the dominant two-body forces along a chain of interparticle vectors, where the KS method is applied to the pair-wise attractions; then, contributions from secondary interactions are added to the dominant ones.
Chain regularisation has been improved by means of the slow-down procedure, which exploits the principle of adiabatic invariance both to scale small physical perturbations by a factor greater than one, so that an orbit may represent several Kepler orbits, and to study short-period binaries in a more accurate manner.
However, chain regularisation proves inefficient in the case of black-hole binaries, which are characterised by high mass ratios, for their binding energy constitutes the prevailing component of the total subsystem energy. Thus in this case chain regularisation is replaced by the time-transformed leapfrog scheme.

## 4.3 Initial setup

In order to put constraints on the dynamical evolution of star clusters, the most relevant initial conditions to be selected are the Initial Mass Function (IMF) and the initial density distribution.
As far as the IMF is concerned, the simplest choice for open clusters is a Salpeter-type IMF, which can be reproduced by the power-law:

$$f(M) \propto M^{-\alpha} \tag{4.14}$$

for a specified mass range $[M_1, M_N]$; the exponent typically attains the value $\alpha$=2.3.
The corresponding distribution for each member $i$ of the system is therefore provided by the expression:

$$M_i^{-(\alpha-1)} = M_1^{-(\alpha-1)} - (i-1)g_N \tag{4.15}$$

where:

$$g_N = \left( \frac{M_1^{-(\alpha-1)} - M_N^{-(\alpha-1)}}{N-1} \right) \tag{4.16}$$

A power-law form for the IMF is suitable for two main reasons: the former is that low-mass stars do not represent a large fraction of the total cluster mass, whereas the latter is that massive stars play a major role in the dynamics of small star clusters for they perform a significant mass loss rate on short timescales.
In place of the IMF, the mass generating function by Kroupa, Tout, and Gilmore (1993)

can be assigned:

$$M(x) = 0,08 + \frac{\gamma_1 x^{\gamma_2} + \gamma_3 x^{\gamma_4}}{(1-x)^{0,58}} \tag{4.17}$$

where $x \in [0,1]$ is a random number and $\gamma_i$ are best-fit coefficients according to the chosen environment.

On the other hand, the initial density distribution is usually assumed to be spherical with some degree of central concentration, such as the Plummer sphere:

$$\rho(r) = \frac{3M}{4\pi r_0^3} \frac{1}{[1 + (\frac{r}{r_0})^2]^{\frac{5}{2}}} \tag{4.18}$$

where $r_0$ is a scale factor related to the half-mass radius by the expression $r_h \simeq 1.3 r_0$. Alternatively, a more general King model with varying central density contrast can be selected; however, since King models are characterised by isotropic velocities and are typically truncated at the local escape velocity, a more appropriate choice is given by the King-Richy models, which include velocity anisotropies.

### 4.3.1 Initial conditions for binary and multiple systems

Every $N$-body simulation is assigned a fraction of both primordial binaries and primordial triples at the beginning.
Given as an input parameter the total number of stars $N = N_s + N_b$, where $N_s$ is the number of single stars and $N_b$ the number of primordial binaries, the $2N_b$ component masses for these ones are generated independently: as a consequence, first the sum of pair-wise masses is performed in decreasing order and then the individual values are recorded separately. In the end, the component masses of each binary system are introduced by splitting the relevant centre-of-mass body. In particular, primordial binary components are labelled as $N_i$, $N_j$ in order for them to be distinguished from the exchanged ones.
Instead, the generation of primordial triples consists in splitting the primary masses of primordial binaries in two parts with suitable two-body parameters, so that an inner binary is formed.

After that, significant parameters for the initialisation of primordial binaries are chosen:

- A flat semi-major axis distribution in $\log(a)$, according with the results for low-mass stars in the solar neighbourhood.
- Eccentricities taken from a thermal distribution.

- Appropriately randomised perihelion, node and inclination angle.

Initial conditions for triples are selected depending on the values of the outer pericentre and the eccentricity.

## 4.4 Decision-making

*N*-body simulations involve a large number of decisions, especially regarding complex astrophysical processes: for this reason they are equipped with a flexible framework for decision-making and hence develop suitable criteria to change the integration scheme and identify which procedures should be carried out according to the different scenarios.
Consequently decision-making consists in several operations:

- Selecting the next particle (or block of particles) to be advanced in time.
- Accounting for close encounters, in particular between single stars and either binaries or subsystems containing binaries.
- Treating the escape process in order to determine the exact membership.

which are based on different physical and computational criteria. Hereafter a description of each decision-making operation will be provided.

### 4.4.1 Scheduling

Scheduling is a queuing problem, as it consists in the determination of the next particle(s) to be considered for integration.
In fact, given a distribution of $N$ individual time-steps $\Delta t_j$ and the corresponding time $t_j$, the next particle to be advanced is chosen by means of the criterion:

$$i = min_j\{t_j + \Delta t_j\} \tag{4.19}$$

so that the new time $t = t_i + \Delta t_i$ is obtained. Thus in this way a list $L$ of particles, fulfilling the request $t_j + \Delta t_j < t_L$ and between which the next one is selected, can be created. By implication, anytime this condition is violated, the list is redefined.
Clearly, in the case of block time-steps more particles have to satisfy the specified criterion at once in order to be moved forward. Therefore, an array of particles having $\{\tilde{t_j} \equiv t_j + \Delta t_j\}$ is constructed so that the condition $\{\tilde{t_j}\} = t_{min}$, where $t_{min}$ is the smallest value in the array, identifies which particles to select.

### 4.4.2 Close two-body encounters

Knowing that the timescale for a typical close encounter is:

$$\Delta t_{ce} \simeq 0.4\sqrt{\frac{\eta_I}{0.02}}\sqrt{\frac{R_{ce}^2}{\overline{M}}} \tag{4.20}$$

where $\overline{m}$ is the mean mass and:

$$R_{ce} = \frac{4r_h}{N} \tag{4.21}$$

is the close encounter radius depending on the half-mass radius $r_h$, if a particles $k$ complies the request $\Delta t_k < \Delta t_{ce}$, then a search for the nearby particles can be performed by using the neighbour list. Otherwise, all sorrounding particles need to be considered: in this case every particle inside the distance $2R_{ce}$ is assumed as a potential neighbour and the closest one in labelled by the index $l$.
At this stage, the pair $k$,$l$ is accepted for KS regularisation if both the distance $R$ between the two particles is such that $R < R_{ce}$ and the two-body force becomes dominant as soon as another close particle denoted by the index $j$ is present, so that:

$$\frac{M_k + M_l}{R^2} > \frac{M_l + M_j}{\left|\vec{r}_l - \vec{r}_j\right|^2} \tag{4.22}$$

Nevertheless, since in the event of massive binaries with low eccentricities the condition $\Delta t_k < \Delta t_{ce}$ may proved too conservative for a close encounter search, the new request $M_k > 2\overline{M}$ is added: only if both the requirements are simultaneously satisfied, KS regularisation is carried out.

Termination of KS regularisation is a more difficult issue for decision-making because a distinction between soft and hard binaries has to be made. Hence the conditions for termination in the former case are $R > R_0$ and $\gamma > \gamma_{max}$, where $R_0$ is the initial separation and $\gamma$ is a perturbation parameter such that $\gamma_{max} \simeq 0.01$; instead, in the latter case strong perturbations without exchange of the binary components, which cause $\gamma$ to be particularly high (i.e. $\gamma$=0.2), may be present, so that termination is performed by searching for the perturbing body.

### 4.4.3 Multiple encounters

Despite several techniques to deal with multiple encounters exist, the most interesting one as far as decision-making is concerned is chain regularisation.

Provided that $\Delta t_{cm} < \Delta t_{ce}$, where $\Delta t_{cm}$ is referred to the centre of mass of each system, the following conditions need to be satisfied in order for chain regularisation to start:

- Negative radial velocity for intruders.
- Compactness condition:

$$\left|\vec{R}_{cm} - \vec{R}_j\right| < max\{3R_{grav}, R_{ce}\} \tag{4.23}$$

  where:

$$R_{grav} = \frac{M_k M_l + M_{cm} M_j}{|E_b + E_{out}|} \tag{4.24}$$

  is the characteristic gravitational radius and $E_b, E_{out}$ are the binding energies of the inner and the outer system respectively.

- Condition of small pericentre distance for strong interactions:

$$a_{out}(1 - e_{out}) < |a|\,(1 + e) \tag{4.25}$$

  where $a_{out}$ and $e_{out}$ are the semi-major axis and the eccentricity of the outer system.

Furthermore, chain regularisation may be initiated with four members instead of three if two hard binaries approach each other closely: in this case the second binary is treated as a single particle and its internal energy is added in the binary binding energy $E_b$ which enters the expression for $R_{grav}$. Then, the semi-major axes of the two interacting binaries are summed up due to the enlargement of the apocentre cross section, so that the condition of small pericentre distance can be generalised.

To conclude, decision-making for chain regularisation termination requires a search for escape candidates to be performed after each integration step if:

$$\sum_k R_k > 3R_{grav} \tag{4.26}$$

### 4.4.4 Hierarchical configurations

Hierarchical configurations appear frequently in star clusters where the primordial binary fraction is particularly high and play an important role in their dynamical evolution due to both their being long-lived and their large cross section. In fact, the formation of new binary systems is quite rare compared to that of hierarchical ones: although the few newborn binaries are hard and therefore unlikely to be destroyed

in encounters with single stars, they are typically disrupted when interacting with primordial binaries, which are characterised by higher binding energies. What is more, the generation of high-order systems is allowed in the star cluster post-collapse phase thanks to the decrease of the core density, and is probably driven by either dynamical friction or large density fluctuations.

To cope with several technical problems arisen from the presence of such systems in $N$-body simulations because of the very short periods involved, which prevent the application of direct integration methods as well as of the KS regularisation procedure, a semi-analytical criterion based on the outer pericentre distance $R_p^{out}$ has been implemented:

$$R_p^{crit} = C\left[(1-q_{out})\frac{(1+e_{out})}{\sqrt{1-e_{out}}}\right]^{\frac{2}{5}} a_{in} \tag{4.27}$$

where $C \simeq 2.8$ is an empirically determined constant, $a_{in}$ is the initial semi-major axis, $e_{out}$ is the eccentricity of the outer system and:

$$q_{out} = \frac{M_3}{M_1+M_2} \tag{4.28}$$

is the outer mass ratio. This criterion ensures stability against the escape of the outermost body of the configuration. Moreover, a condition for possible exchanges of the inner components is given by:

$$(\vec{J}^2 E)_{crit} = -\frac{G^2 f^2(\rho) g(\rho)}{2(M_1+M_2+M_3)} \tag{4.29}$$

where $f(\rho), g(\rho)$ are algebraic functions.
If $\vec{J}^2 E < (\vec{J}^2 E)_{crit}$ no exchange can occur and therefore the inner binary retains its identity. However, this condition is only sufficient, not necessary: this means that, in spite of its violation, there may be some exchanges but only if followed by escape.
As for stability, a triple is defined to be stable if $a_{out}(1-e_{out}) > R_p^{crit}$: hence the inner binary does not experience secular effects and short-term fluctuations can be neglected. On the other hand, quadruples and higher-order systems can be treated in a similar fashion, provided that appropriate corrections to the stability criterion are introduced.

### 4.4.5 Escapers

Since star clusters evolve by losing members to the Galactic field, $N$-body simulations make use of various criteria to account for escapers and thus determine the exact

membership at any given time. In fact, star clusters orbiting the Galaxy are subjected to an external tidal field which is responsible for the increase of the stars disruption rate: hence the inclusion of the concept of tidal radius, i.e. the radius beyond which stars are no more gravitationally bound to the system and therefore fated to escape in a considerably short timescale.
However, the tidal radius $r_t$ is not always the best choice for the identification of the cluster boundary, as $N$-body simulations have shown that a significant population beyond this limit may be present; also, theoretical considerations suggest that some orbits may reach large distances but then return to the cluster, so that stars moving along them are not lost.
Consequently, another escape criterion has been proposed:

$$|\vec{r}_i - \vec{r}_d| > 2r_t \tag{4.30}$$

where $\vec{r}_d$ defines the density centre. So, when this condition is fulfilled, stars are removed and the new total number $N$ of members is calculated.
Finally, it is worth pointing out that escape from stellar systems can be caused either by close encounters (ejection) or by the cumulative effect of many small encounters (evaporation); in particular, ejection is less important in rich clusters dominated by single stars, for close encounters typically involve binaries.

## 4.5 Star cluster simulations

The evolution of self-gravitating systems is typically articulated by the crossing timescale:

$$t_{cross} = \frac{2r_v}{\sigma} \tag{4.31}$$

where:

$$r_v = \frac{GN^2\overline{M}^2}{\sigma 2\,|U|} \tag{4.32}$$

is the virial radius derived from the expression for the potential energy and $\sigma$ is the velocity dispersion. Nevertheless, the half-mass relaxation time is more useful as far as star cluster simulations are concerned, since it is not sensitive to the density profile:

$$t_{relax,hm} = 0.138\sqrt{\frac{Nr_{hm}^3}{Gm}}\frac{1}{\ln(\gamma N)} \tag{4.33}$$

where $r_{hm}$ is the half-mass radius and $\gamma$ is a parameter whose most usual value is $\gamma \simeq 0.4$.
If, on the one hand, $t_{cross}$ is the timescale for a stellar system to adjust globally from any significant deviation from the virial equilibrium, on the other $t_{relax,hm}$ is the time for a velocity change to become comparable to the initial velocity dispersion $\sigma_{in}$: as a consequence, $t_{relax,hm}$ can be addressed as a reference time for dynamical changes affecting the whole cluster.

*N*-body simulations of evolving star clusters can be either idealised or realistic; in particular, idealised simulations are employed for three main purposes:

- Making comparisons through approximate methods.
- Modelling astrophysical processes.
- Investigating dynamical processes (i.e. escape, binary and multiple systems formation).

However, they can be turned into realistic by adding some elements, such as an IMF and a fraction of primordial binaries.

### 4.5.1 Initial mass function

The IMF is a fundamental tool to conduct research about the dynamical evolution of star clusters as it introduces a mass spectrum and therefore evaluates the contribution from different masses.
The choice of an IMF for star cluster simulations is generally guided by observations of young systems, i.e. open clusters; in consequence, the classical Salpeter-type IMF may not be appropriate: in fact, it has been found that the distribution of low-mass stars is significantly depleted with respect to that expected from a power-law IMF with index $\alpha = 2.3$.
Besides, the maximum mass incorporated in the IMF is rather arbitrary, but it seems that a conservative value of 15 $M_{\odot}$ is suitable for open clusters, even though bigger values can be chosen as theoretically allowed.

### 4.5.2 Primordial binaries

Including primordial binaries in star clusters simulations immediately shows their importance in regard to dynamics. In fact, just a small fraction of primordial binaries has been demonstrated to be enough to affect the cluster evolution significantly once

an IMF is chosen and stellar evolution is appropriately taken into account: this is due to the fact that the most massive stars are depleted first via stellar evolution, so that the central concentration of binaries steadily increases. By implication, they are left to play a major role in dynamical processes, i.e. two-body relaxation.
This means that the presence of binaries tends to enhance the rate of stellar collisions and close encounters, which can lead to the formation of both multiple and new binary systems. Furthermore, binary encounters are responsible for a spread in the energy distribution, with hard binaries experiencing a small energy change with respect to soft ones. Therefore, it follows that the encounters with soft binaries provide a source of fuel to halt the collapse of the cluster core, whereas those with hard ones are likely to produce high-velocity escapers.

## 4.6 *N*-body simulations employed in this work

### 4.6.1 Structure and initial conditions

In the aim of studying the impact of binary stars on the estimate of the total mass of stellar systems, three open-cluster-like models have been realised by means of *N*-body simulations performed with the code *NBODY7*, which has been developed by Nitadori and Aarseth (2012). In fact, *NBODY7* not only permits a reliable integration of the motion of stars through state-of-the-art methods such as regularisation, but also implements careful treatments to deal with relevant astrophysical processes, i.e. close encounters, stellar evolution, mass loss and escape. Therefore it proves particularly suitable for the analysis of star clusters dynamics. Each model has been assigned an initial number of stars $N_{in}$=1000 and an initial mass $M_{in}\sim$6-7$\times10^2$ $M_\odot$; then, a Plummer density profile (Plummer 1911) and a Kroupa IMF (Kroupa 2001):

$$f(M) \propto M^{-\alpha} \tag{4.34}$$

with exponent $\alpha$=0.3 for $M$<0.08 $M_\odot$, $\alpha$=1.3 for 0.8 $M_\odot$<$M$<0.5 $M_\odot$, $\alpha$=2.3 for $M$>0.5 $M_\odot$ and masses in the range 0.01 $M_\odot\leq M\leq$100 $M_\odot$ have been selected. The cluster core radius is of the order of $r_c$=1 pc, whereas the metallicity is assumed to be solar (Z=0.0).
Moreover, the simulated clusters are considered both isolated and in virial equilibrium and have been evolved up to ∼3 Gyr (Model A) and ∼2.5 Gyr (Model B, Model C).

All the models share the same characteristics apart from the initial binary fraction: in particular, Model A contains 50 primordial binaries (5%), Model B 150 primordial binaries (15%) and Model C 300 primordial binaries (30%).

Each primordial binary population has been modelled by adopting equal distributions though, i.e. a logarithmic period distribution, a thermal eccentricity distribution *f(e)*=2*e* and a mass-ratio distribution:

$$f(q) \propto q^{0.4} \tag{4.35}$$

Thus the choice of varying the initial binary fraction only is intended to evaluate their very influence on the parameters describing the environment which they belong to.

### 4.6.2 Results

A thorough analysis of the outputs of the *N*-body simulations for each model has been performed.
To begin with, the dependence of the total cluster mass on time has been investigated (Fig. 4.1).
It is evident that the total mass drops during the first few hundreds of Myrs, i.e. up to ∼100 Myr for Model A, ∼500 Myr for Model B and ∼200 Myr for Model C, but decreases less sharply from ∼1000 Myr onward in all the models.
This trend is due to mass loss from stellar evolution, which is of greatest importance in the initial phases of cluster evolution: in fact, the rapid depletion of high-mass stars typically results in a substantial reduction of the cluster mass and can actually cause the dissolution of the cluster itself.
However, if a stellar system is able to survive this early stage, then stellar evolutionary timescales tend to grow longer compared to those for dynamical evolution, so that two-body relaxation and tidal effects become dominant. Therefore, further mass is lost in form of escaping stars after close encounters, especially when an external tidal field is present: by implication, clusters in virial equilibrium, such as the ones here examined, are not significantly affected by this process for they are isolated.
On the other hand, mass loss can be promoted by primordial binary systems, since they tend to enhance the number of stellar collisions: thus it follows that they may be either destroyed in strong interactions or form new configurations by exchanging their components with single stars or other binaries in close encounters. In particular, the disruption rate of primordial binaries is generally less pronounced in open clusters, as strong interactions in such environments are quite rare.
For this reason, it is likely that primordial binary systems play a major role in powering cluster mass loss after stellar evolution in the models.

In order to evaluate binary dynamics throughout the models, the time evolution of the binary fraction:

$$f_b(t) = \frac{N_b(t)}{N(t)} = \frac{N_b(t)}{N_s(t) + N_b(t)} \tag{4.36}$$

has been displayed. Except for Model A, which shows a slight increase of the binary fraction from the initial time up to ∼500 Myr and then a progressive decrease, the other models are characterised by a continuous and steeper decline: thus the number of primordial binary systems tends to diminish as soon as they are subjected to dynamical interactions, i.e. close encounters and tidal captures, which lead either to the destruction or to the modification of the original configurations.
Even so, there are some growth peaks in the graphs, representing the new binary systems formed during such interactions, especially after exchanges (Fig. 4.2).

As a consequence, a statistics about the dynamical events primordial binary systems experience in each model has been performed: the number of both destructions ($N_{destructions}$) and exchanges with either single stars or other binaries ($N_{exchanges}$) has been computed, together with the number of newborn binary systems ($N_{b,new}$).
Moreover, the survival rate, i.e. the number of primordial binaries remained unaltered from the beginning to end of the simulations, and the final normalised binary fraction, i.e. the ratio between the number of binaries at the final time and that at the initial time:

$$f_{b,norm}(t_{fin}) = \frac{N_b(t_{fin})}{N_b(0)} \tag{4.37}$$

have been calculated. The results are listed in Tab. 4.1:

| | $N_{destructions}$ | $N_{exchanges}$ | $N_{b,new}$ | *Survival rate* | $f_{b,norm}(t_{fin})$ |
|---|---|---|---|---|---|
| *Model A* | 16 | 1 | 4 | 76% | 0,76 |
| *Model B* | 47 | 14 | 12 | 73% | 0,75 |
| *Model C* | 64 | 5 | 10 | 82% | 0,82 |

Table 4.1: Binary dynamics statistics.

suggesting that the higher the fraction of primordial binaries, the richer their dynamical history. In fact, the number of destructions increases going from Model A to Model C, whereas the number of exchanges seems to be related to that of newborn binary systems. On the contrary, neither the survival rate nor the normalised binary fraction show a particular dependence on the initial number of binaries.
Inter alia, a search for tidal capture events has been made by looking at the formation of temporary triples: primordial binary systems occurring at a time and then disappearing to show up again in the original configuration some Myrs later in the simulations have been identified as temporary triples, since the presence of the third star comes as a time-limited perturbation. However, these events have been found to be rare in all models.

In conclusion, the trend of the various parameters discussed above as a function of time has been plotted to confirm the results (Fig. 4.3).

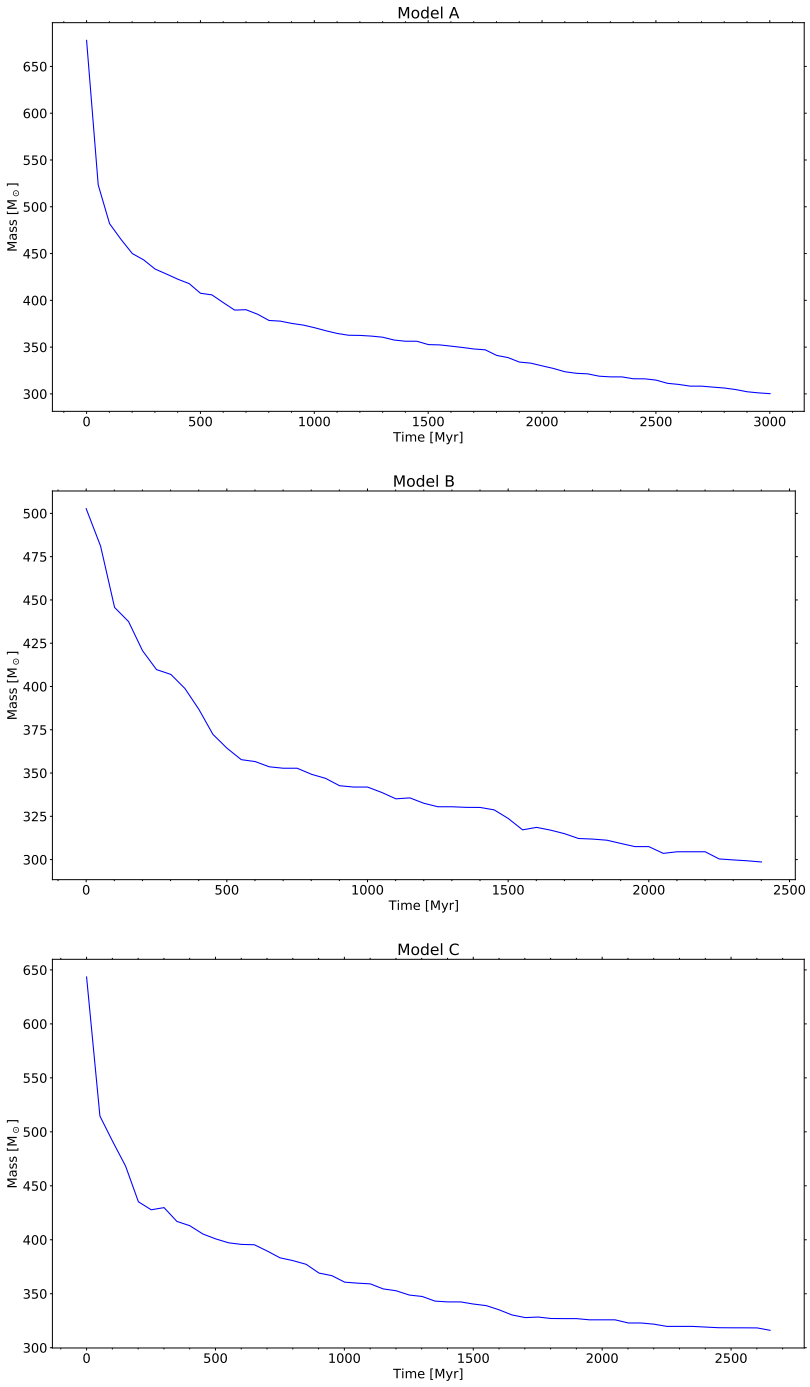


Figure 4.1: Total cluster mass as a function of time.

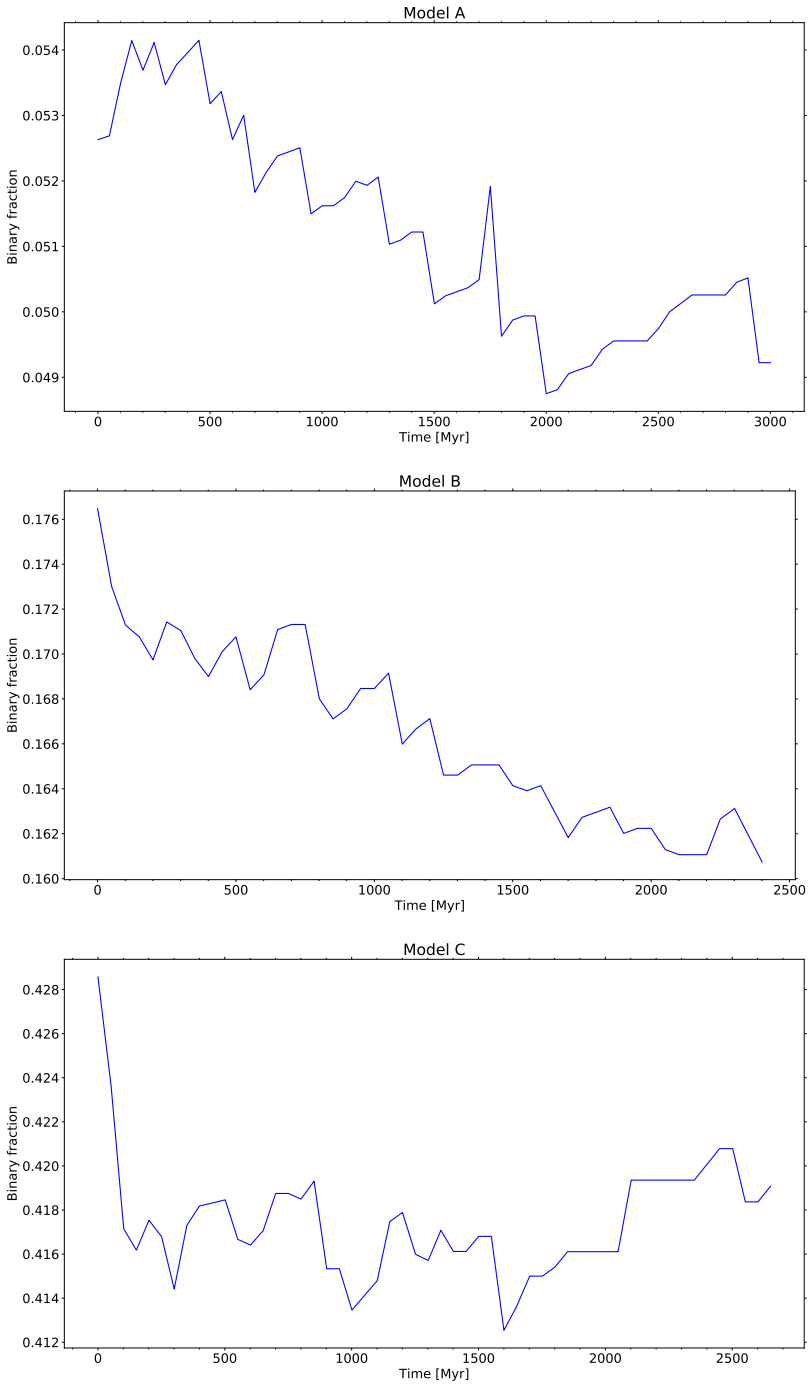


Figure 4.2: Binary fraction as a function of time.

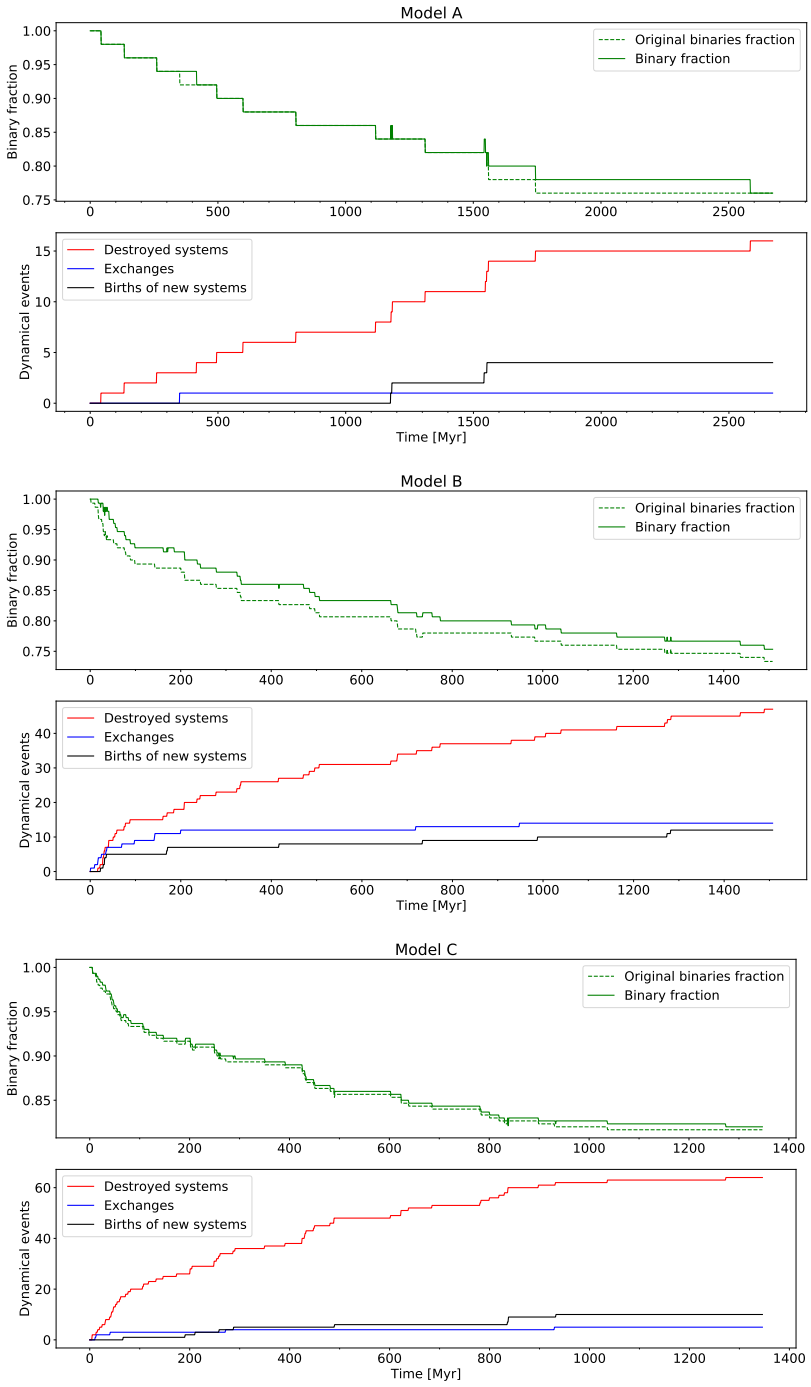


Figure 4.3: Binary dynamical events as a function of time.

# Chapter V

# Binary stars and total cluster mass estimates

The presence of binary stars has a strong impact on the total mass of stellar systems, as neglecting binaries leads to unequivocally wrong mass estimates.
With the goal of highlighting this fact, two different methods based on the Hertzsprung-Russel diagram (HRD) have been selected for the computation of the total cluster mass: both the procedures are intended to put in evidence the effects of not taking account for binaries properly, thus they simulate typical mistakes which could be made on this matter.

A HRD at the age of 2.4 Gyr has been realised for each model by considering all the single stars and all the binary systems listed in the simulations outputs (Fig. 5.1): the binary sequence is placed on the right of the cluster MS, clearly detached from it, even though some binaries populate the MS itself; in particular, the binary sequence is composed of equal-mass binaries ($q$=1), whereas the cluster MS contains those having more massive primaries ($q \longrightarrow 0$). In the end, few binary systems can be detected also in the bottom-left part of the diagrams, where dwarf stars are located.

As a reference for the results of the two methods, the theoretical mass $M_{th}$ has been calculated by summing up the masses of every single star and binary component tabulated in the models (Tab. 5.1): hence $M_{th}$ can be regarded as the real cluster mass, i.e. the mass the cluster would have if all its members were resolved.

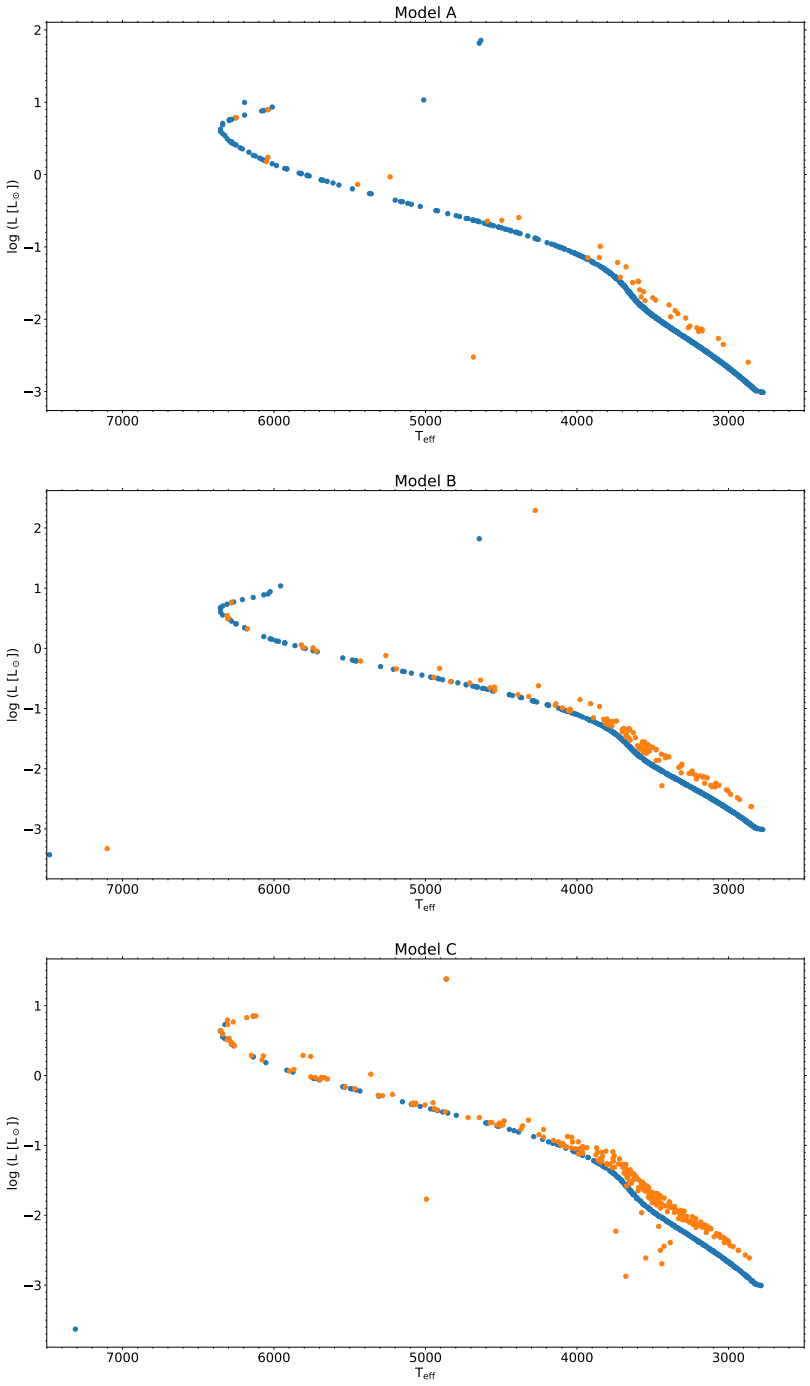


Figure 5.1: Hertzsprung-Russell diagrams.

| | $M_{th}$ |
|---|---|
| *Model A* | 316.1 $M_\odot$ |
| *Model B* | 298.6 $M_\odot$ |
| *Model C* | 318.2 $M_\odot$ |

Table 5.1: Theoretical cluster mass.

## 5.1 Photometric method

The so called photometric method typically relies on the luminosity function (LF), which can be actually regarded as a luminosity distribution for it returns the stellar number density, i.e. the number of stars, per luminosity interval. Therefore, assuming absolute stellar magnitudes in the $V$ band for instance, the number of stars with absolute magnitude $V \in [V, V+\Delta V]$ is given by:

$$N = \int_V^{V+\Delta V} \phi(V) dV \tag{5.1}$$

where $\phi(V)$ is exactly the LF.
The LF can be determined by using either a standard histogram technique or a kernel estimator method.
In the former case, first the observed stellar magnitudes are transformed in absolute magnitudes by means of the cluster distance and the colour excess, and then the resulting absolute magnitude distribution is binned in intervals, usually tuned in order to get at least one star per interval. Finally, the number of both single and binary stars in each bin:

$$N_s = \int_V^{V+\Delta V} \phi(V) dV \quad , \quad N_b = f_b(t) \int_V^{V+\Delta V} \phi(V) dV \tag{5.2}$$

where $f_b(t)$ is the binary fraction, is counted and stellar absolute magnitudes are converted into luminosities starting from the selected isochrone for the cluster age.
In this way, a histogram composed of luminosity bins collecting stars can be constructed.
Instead, in the latter case a kernel estimator in the form of a continuous function in one dimension (Seleznev 1998) is introduced:

$$\hat{f}(x) = \frac{1}{nh} \sum_{i=1}^{n} k\left(\frac{x - X_i}{h}\right) \tag{5.3}$$

where $n$ is the size of the observed sample $X_1, ..., X_n$ of the random variable $x$, $h$ is the interval width and $k\left(\frac{x-X_i}{h}\right)$ is the kernel function, which is mainly assumed to be a symmetric probability distribution, i.e. a normal distribution, satisfying the relation:

$$\int_{-\infty}^{+\infty} k(x)dx \tag{5.4}$$

Also, an adaptive kernel estimator can be adopted:

$$\hat{f}(x) = \frac{1}{n}\sum_{i=1}^{n} h\lambda_i k\left(\frac{x - X_i}{h\lambda_i}\right) \tag{5.5}$$

where the interval width $h\lambda_i$ differs from point to point and:

$$\lambda_i = \left(\frac{\tilde{f}(X_i)}{g}\right)^{-\alpha} \tag{5.6}$$

with $\alpha \in [0,1]$, are the local width factors. In addition, $\tilde{f}(X_i)$ such that $\tilde{f}(X_i) > 0 \ \forall i$ and characterised by the logarithmic mean:

$$\log(g) = \frac{1}{n}\sum_{i=1}^{n} \log(\tilde{f}(X_i)) \tag{5.7}$$

is a preliminary estimate obtained by way of a fixed kernel estimator.
In particular, according to Prisinzano et al. (2001) the adaptive kernel estimator method has the following advantages with respect to the standard histogram technique:

- The definition of a bin, whose size is mostly arbitrary and inconvenient for the detection of all the statistically relevant features of the CMD, is not necessary.
- The histogram depends on both the bin and the initial bin location, whereas the kernel estimator depends only on the interval width.

Since the cluster LF has to be corrected for incompleteness, a LF is generally calculated for different fields, i.e. for different regions of the CMD: the LFs of the external fields are therefore used to subtract the field-star contamination from the LF of the central field.
As an illustration, Seleznev et al. (2017) made use of this procedure to determine the mass of the Galactic open cluster NGC 4337, thus succeeding in constraining the cluster LF (Fig. 5.2).

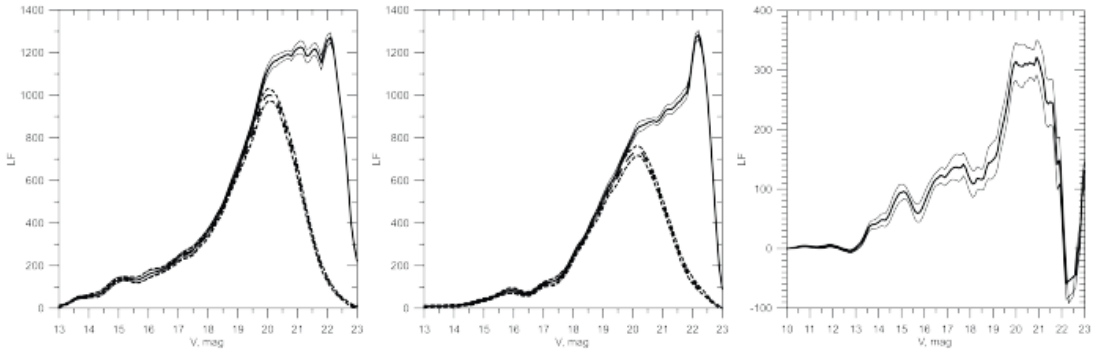


Figure 5.2: Left panel: LF for cluster regions both corrected (solid line) and uncorrected (dashed line) for incompleteness. Middle panel: LF for field regions both corrected (solid line) and uncorrected (dashed lines) for incompleteness. Right panel: Cluster LF, the result of subtraction of the field LF from the cluster region LF.

Here the photometric method has been employed under the hypothesis of all the binaries being unresolved, so that they have been treated as single stars.

This scenario is typical of old and massive Galactic open clusters, in which both the contamination by a significant number of field stars and the presence of binaries are responsible for such a struggle in the mass computation that no other means but looking at the appearance of the colour-magnitude diagram (CMD) are left to use.
As an example, in the case of the oldest Galactic open cluster Melotte 66 (Fig. 5.3), i.e. $3.4 \pm 0.2$ Gyr old according to Carraro et al. (2014), it took several years from the first realisation of its CMD (Hawarden 1976) to discover a binary sequence on the right side of the cluster MS, intersecting it close to the turn-off (TO) and causing its broadening (Zloczewski et al. 2007).
However, despite the improvement of the CMD appearence through the medium of very deep CCD photometry, binary resolution resulted still difficult: for this reason a cluster sharing the same characteristics as Melotte 66, but with the addition of a fraction of 30% binary stars, has been simulated and thus a synthetic CMD created (Carraro et al. 2014). Since the real CMD was well reproduced by the synthetic one, the conclusion of binaries being fundamental in the cluster analysis has been drawn.

Given the objective of a purely theoretical demonstration, in this instance the photometric method has been directly applied to the HRD, without passing through the LF calculation.
If all the stars are considered as single, then their luminosity can be inferred from the corresponding ordinate in the HRD; hence, in order to transform the luminosity into mass, the mass-luminosity relation proposed by Borodina et al. (2019) for MS stars has

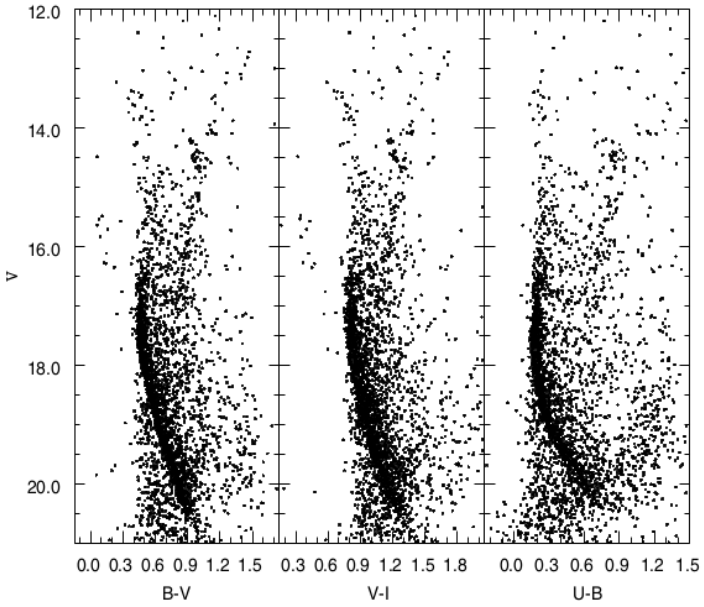


Figure 5.3: Melotte 66 CMD for different colour combinations.

been adopted:

$$\left(\frac{L}{L_{\odot}}\right) \sim \left(\frac{M}{M_{\odot}}\right)^{4} \tag{5.8}$$

In this way, every point in the HRDs has been assigned its own mass. All the masses thus obtained have been summed to compute the total cluster mass for each model, i.e. the photometric mass $M_{phot}$, which has been subsequently compared to the theoretical mass $M_{th}$: to this purpose, both the absolute error:

$$E_{abs,phot} = \left|M_{phot} - M_{th}\right| \tag{5.9}$$

and the relative error:

$$E_{rel,phot} = \left|\frac{E_{abs,phot}}{100 M_{th}}\right| \tag{5.10}$$

have been calculated.
As expected from the relation:

$$M_s^4 < (M_1 + M_2)^4 \Longrightarrow M_s < M_1 + M_2 \tag{5.11}$$

where $M_s$ indicates the mass of single stars, whereas $M_1$ and $M_2$ the mass of the primary and the secondary component of binary systems, $M_{phot}$ should result systema-

tically smaller than $M_{th}$: therefore ignoring the presence of binaries would lead to an underestimation of the total cluster mass.
However, in Model A this does not occur, since $M_{phot}>M_{th}$ due to the very low primordial binary fraction: if the number of binaries is not large enough compared to that of single stars, their effect in the cluster mass underestimation can be minimal. In fact, by isolating the contribution from real single stars to both $M_{phot}$ ($M_{phot,s}$) and $M_{th}$ ($M_{th,s}$), it becomes apparent that in each model $M_{phot,s}>M_{th,s}$: hence single stars are likely to enhance the total cluster mass in the photometric method because of the adopted mass-luminosity relation, which goes like $M^4$. As soon as the contribution of binaries is added to both $M_{th,s}$ and $M_{phot,s}$ to get $M_{th}$ and $M_{phot}$ respectively, this one ends up to be smaller than $M_{th}$ in Model B and Model C consistently to the increasing primordial binary fraction (Tab. 5.2): the higher the initial binary fraction, the greater the difference between $M_{phot}$ and $M_{th}$.

| | $M_{th,s}$ | $M_{phot,s}$ | $M_{th}$ | $M_{phot}$ | $E_{abs,phot}$ | $E_{rel,phot}$ |
|---|---|---|---|---|---|---|
| *Model A* | 287.2 $M_\odot$ | 310.7 $M_\odot$ | 316.1 $M_\odot$ | 331.2 $M_\odot$ | 15.1 | 4.7% |
| *Model B* | 216.1 $M_\odot$ | 233.6 $M_\odot$ | 298.6 $M_\odot$ | 293.9 $M_\odot$ | 4.7 | 1.6% |
| *Model C* | 127.8 $M_\odot$ | 135.4 $M_\odot$ | 318.2 $M_\odot$ | 266.7 $M_\odot$ | 51.5 | 16.2% |

Table 5.2: Comparison between the photometric and the theoretical mass obtained from real single stars ( i.e. $M_{phot,s}$ and $M_{th,s}$) and from both single and binary stars (i.e. the total cluster photometric mass $M_{phot}$ and theoretical mass $M_{th}$), together with the errors for $M_{phot}$.

Notably, $E_{rel,phot}$ attains a lower value in Model B with respect to both Model A and Model C. This result can be easily explained by admitting that Model B reproduces the physical features of the environment where the mass-luminosity relation has been calibrated at best, including the primordial binary fraction: in fact, $E_{rel,phot}$ grows proportionally to the deviation from the initial binary percentage of 15%.

## 5.2 Isochrone fitting method

The isochrone fitting method exploits isochrones, which are curves on the HRD representing stars of the same age, i.e. single stellar populations, to derive the total cluster mass: in fact, isochrones matching the cluster age are able to fit not only the TO but also the MS, thus allowing both to distinguish the vast majority of single stars from binary stars lying in the parallel sequence and to compute the mass of the two species properly.
For this reason an isochrone for the age of 2.4 Gyr and the solar metallicity $Z$=0.0 has

first been selected from the database MIST (Dotter 2016, Choi et al. 2016, Paxton et al. 2011, Paxton et al. 2013, Paxton et al. 2015, Paxton et al. 2018) and then applied to the cluster HRD for each model in order to fit single stars (Fig. 5.4).

In order to account for the progressive broadening of the HRD from the TO to the low MS, a softly increasing exponential error:

$$E_{iso} = Ae^{nT_{eff}} \tag{5.12}$$

with $A$=0.154, $n$= $-1.732 \times 10^{-3}$ and $T_{eff}\in$[2500 K, 6500 K] has been associated to the isochrone fit; in this way, $E_{iso}$=0.05 at $T_{eff}\simeq$6500 K, where the TO is located, and $E_{iso}$=0.1 at $T_{eff}\simeq$2500 K, which marks approximately the end of the MS.
Therefore, stars lying inside the exponential error bars have been treated as single, so that their mass have been calculated by means of the mass-luminosity relation:

$$\left(\frac{L}{L_{\odot}}\right) \sim \left(\frac{M}{M_{\odot}}\right)^{4} \tag{5.13}$$

valid for MS stars (Borodina et al. 2019). In the end, all the masses have been summed up to get the total single-stellar mass $M_s$.
On the other hand, stars not belonging to the isochrone have been regarded as binaries, hence their mass have been estimated in a different fashion.
Two magnitude intervals, the former shifted by $\Delta V$=0.375 and the latter by $\Delta V$=0.75 respectively from the error bars delimiting the single-star locus in the HRD, have been created and assigned a value of the mass ratio $q$: as a result, $q$=0 at the exponential error bars, $q$=0.5 at $\Delta V$=0.375 and $q$=1 at $\Delta V$=0.75. Subsequently, a mean value of $q$ has been calculated for each interval, so that, on both sides of the isochrone, binaries falling inside the first interval have $\overline{q}$=0.25 (low-$q$ binaries) and those inside the second one have $\overline{q}$=0.75 (high-$q$ binaries).
So, in the aim of computing the total mass of each binary system $M_{tot,b}$ the following system of mathematical equations has been introduced and solved for the various values of $\overline{q}$:

$$\begin{cases} \overline{q} = \frac{M_2}{M_1} \Longrightarrow M_2 = \overline{q} M_1 \\ L_1 = M_1^4 \Longrightarrow M_1 = L_1^{\frac{1}{4}} \\ L_2 = M_2^4 \Longrightarrow M_2 = L_2^{\frac{1}{4}} \\ \left(\frac{L_2}{L_1}\right)^{\frac{1}{4}} = \left(\frac{M_2}{M_1}\right) = \overline{q} \Longrightarrow \frac{L_2}{L_1} = \overline{q}^4 \Longrightarrow L_2 = \overline{q}^4 L_1 \\ L_{tot,b} = L_1 + L_2 = L_1 + \overline{q}^4 L_1 = \left(1 + \overline{q}^4\right) L_1 \Longrightarrow L_1 = \left(1 + \overline{q}^4\right)^{\frac{1}{4}} L_{tot,b} \\ M_{tot,b} = M_1 + M_2 = M_1 + \overline{q} M_1 = (1 + \overline{q}) M_1 = (1 + \overline{q}) L_1^{\frac{1}{4}} = \frac{(1+\overline{q})}{\left(1+\overline{q}^4\right)^{\frac{1}{4}}} L_{tot,b} \end{cases}$$

In particular, every binary component in the intervals has been assumed to behave as a single MS star once detached from the original system: thus the mass-luminosity relation for MS stars have been applied to compute the mass of both the primary ($M_1$) and the secondary component ($M_2$), being their luminosity inferred from the HRD.
The masses of all the binaries inside the first interval and of those inside the second interval on both sides of the isochrone have been summed, hence obtaining $M_{b,1}$ and $M_{b,2}$ respectively.
The total cluster mass by the isochrone fitting method $M_{iso}$ has been calculated as the sum of $M_s$, $M_{b,1}$ and $M_{b,2}$ for each model and compared to the theoretical cluster mass $M_{th}$. To conclude, since in this case the total cluster mass has been accomplished via star counts of both single and binary stars in the different magnitude intervals constructed, a Poisson error:

$$E_{poiss} = \sqrt{M_{iso}} \tag{5.14}$$

has been associated to each value of $M_{iso}$ (Tab. 5.3).

| | $M_s$ | $M_{b,1}$ | $M_{b,2}$ | $M_{iso}$ | $E_{poiss}$ | $M_{th}$ |
|---|---|---|---|---|---|---|
| *Model A* | 231.6 $M_\odot$ | 107.9 $M_\odot$ | 11.8 $M_\odot$ | 351.4 $M_\odot$ | 18.74 | 316.1 $M_\odot$ |
| *Model B* | 185.3 $M_\odot$ | 130.1 $M_\odot$ | 28.4 $M_\odot$ | 343.7 $M_\odot$ | 18.5 | 298.6 $M_\odot$ |
| *Model C* | 113.9 $M_\odot$ | 125.2 $M_\odot$ | 64.1 $M_\odot$ | 303.2 $M_\odot$ | 17.4 | 318.2 $M_\odot$ |

Table 5.3: Comparison between the total cluster mass obtained through the isochrone fitting method $M_{iso}$, with the paired Poisson error, and the theoretical cluster mass $M_{th}$.

In order to interpret the results of the isochrone fitting method correctly, a confusion matrix has been produced: the rows represent the predicted values, whereas the columns the actual values, of the number of stars in each interval (Fig. 5.5). In particular, the instance "Other" groups stars which do not belong to any interval and remain cut out because the algorithm is not able to classify them: this is the case

of white dwarfs (WDs), both single and part of binary systems, being them placed in different regions of the HRD. According to the confusion matrix, both in Model A and in Model B several single stars have been labelled as low-$q$ binaries, namely binaries located in the first magnitude interval on both sides of the isochrone, but only few binary systems have not been ranked correctly: thus it appears that the exponential error bars set up in the method are not large enough to contain all single MS stars. This clearly ends up in an overestimation of the total cluster mass due to the mass-luminosity relation employed to derive single-stellar masses, since properly classified single stars outnumber mislabelled single stars and low-$q$ binaries as well.
On the other hand, Model C is characterised by a less precise prediction of the number of both low-$q$ and high-$q$ binaries, which is likely to be linked to the higher initial binary fraction: the greater the number of binary systems, the more difficult disentangling them not only from single stars, but also from each other on the basis of their mass ratio. As a consequence, the fact that many binary stars have been classified as single may outshine the overestimating effect of real single stars over the total cluster mass to such an extent to produce an underestimation of it. This scenario comes about exactly in Model C, for the number of real single stars recognised by the algorithm is lower compared to that of the other models: in fact, if single stars are less numerous, then the role of binaries as regards the cluster mass estimate tends to become dominant.

In the end, it is noteworthy that on the basis of the isochrone fitting method Model C yields the most reliable estimate of the total cluster mass, since the Poisson error associated to $M_{iso}$ attains a smaller value with respect to both Model A and Model B, even though the confusion matrix points out that the overall stellar classification is less accurate: this happens only because the Poisson error depends on $M_{iso}$ in such a way that the higher $M_{iso}$, the higher also $E_{poiss}$.
In fact, by computing the accuracy of the isochrone fitting method for each model as the ratio of the sum of the diagonal values and the sum of all the values in the confusion matrix, it turns out that Model C is the less accountable one in favour of Model B, which seems to be the most representative one in accordance with the photometric method (Tab. 5.4).

| | *Accuracy* |
|---|---|
| *Model A* | 80% |
| *Model B* | 83% |
| *Model C* | 78% |

Table 5.4: Accuracy of the isochrone fitting method.

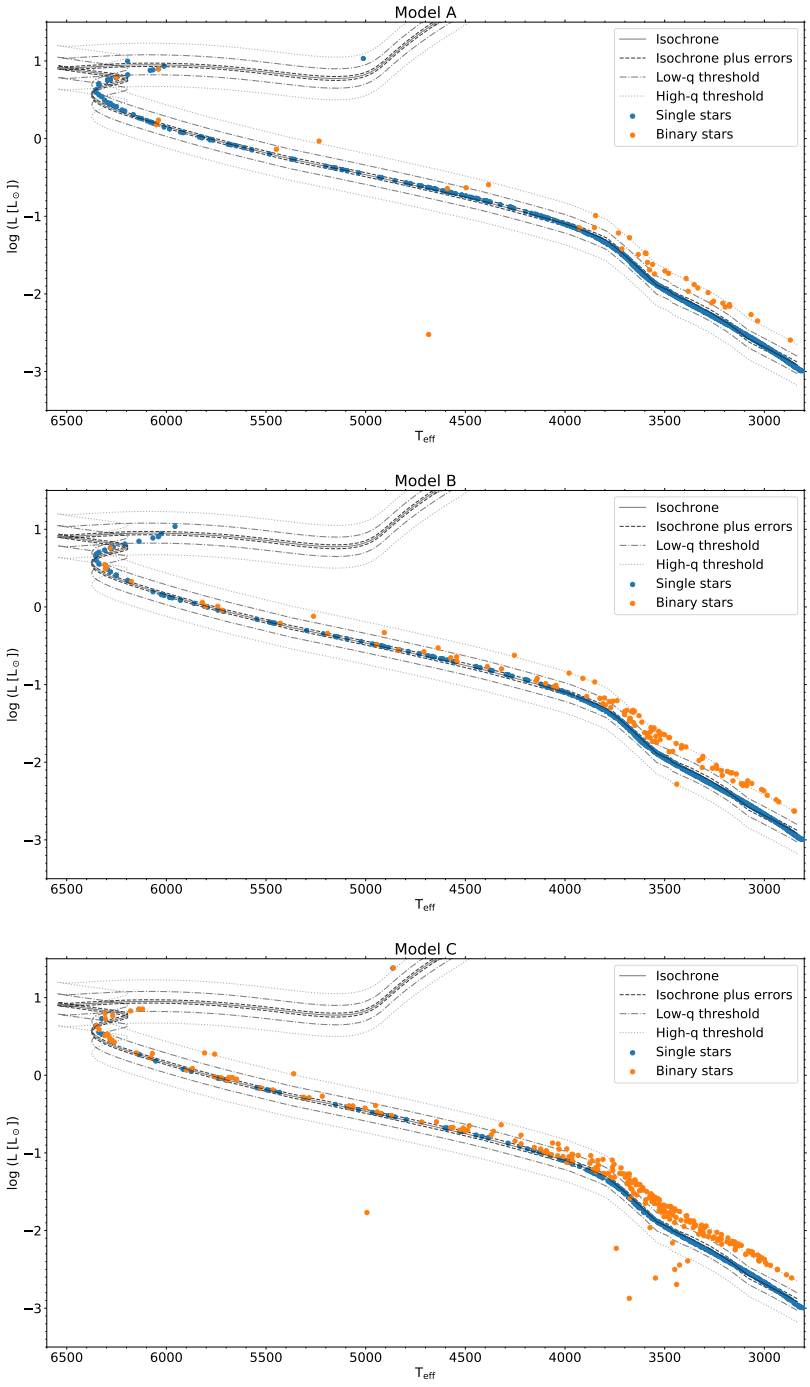


Figure 5.4: Isochrone fit: the solid lines trace isochrones, whereas the dashed lines indicate the exponential error bars. Outside, the threshold of the magnitude intervals for both low-$q$ and high-$q$ binaries is represented.

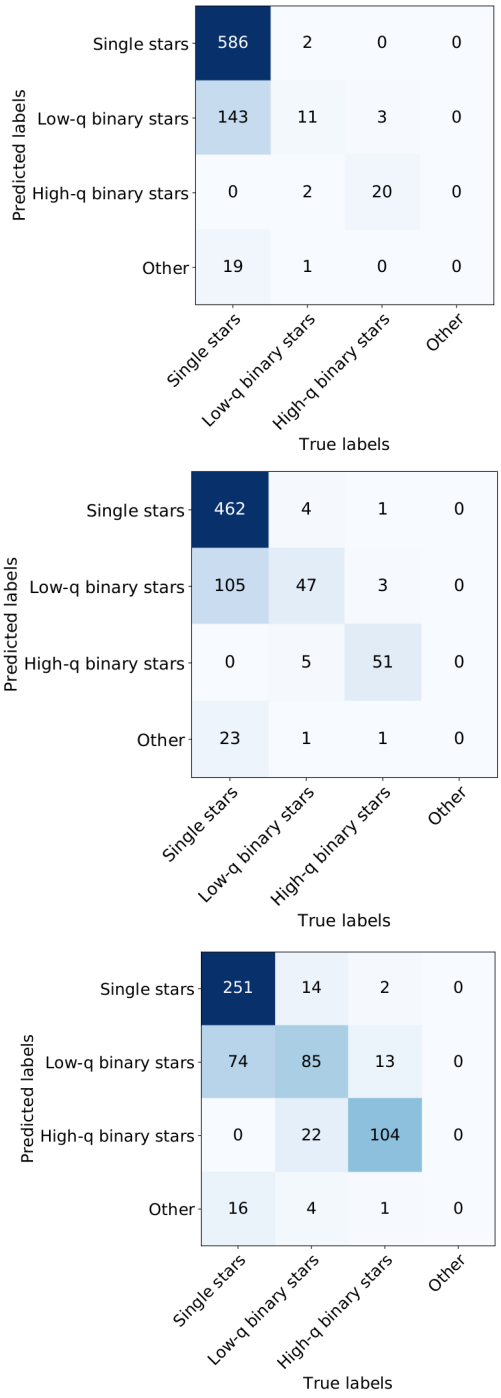


Figure 5.5: Confusion matrix for Model A, Model B and Model C.

# Chapter VI

# Conclusions

The impact of binary stars in the determination of the total mass of stellar systems has been investigated by means of *N*-body simulations in this work.
Since both observations and numerical simulations have pointed out that the presence of binaries in stellar systems such as star clusters cannot be explained by dynamical formation processes, i.e. multiple encounters and tidal captures (Aarseth and Lecar 1975, Binney and Tremaine 2008), it appears that the vast majority must be primordial (Hut et al. 1992), namely formed together with single stars at the cluster birth: thus the initial binary fraction is crucial as far as cluster dynamics is concerned.
Moreover, binaries are far more common in open clusters with respect to globular clusters for they tend to survive longer in loosely bound environments, where strong interactions are rare: in fact, the initial binary fraction in GCs is significantly reduced because of close encounters taking place in their cores during their dynamical evolution (Ji and Bregman 2013).
For this reason three open-cluster-like *N*-body simulations with a different primordial binary percentage have been realised (Model A: $f_b(0)$=5%, Model B: $f_b(0)$=15%, Model C: $f_b(0)$=30%), returning the following results:

- The total cluster mass decreases as a function of time in all models, with a sharp drop during the first few hundreds of Myrs due to stellar evolution, which predict a rapid depletion of high-mass stars in the initial phases of cluster evolution. Further mass is lost both in form of escaping stars after close encounters and as a consequence of the presence of binaries, which enhance the stellar collision rate.

- The binary fraction $f_b(t)$ declines in time as soon as binaries are subjected to dynamical interactions, i.e. close encounters and tidal captures, which lead either to the destruction or to the modification of the original systems.

- A statistics about binary dynamical events, i.e. destructions, exchanges and formation of new binary systems after close encounters, has shown that the higher the fraction of primordial binaries, the richer the cluster dynamical history. In fact, the number of destructions grows consistently with the initial binary fraction, whereas the number of exchanges seems to be related to that of newborn binary systems. On the other hand, no specific dependence of the survival rate on the primordial binary fraction has been found.

- Very few temporary triples have been identified.

Then two different methods, i.e. the photometric and the isochrone fitting methods, to compute the total cluster mass have been applied to the HRD at the age of 2.4 Gyr for each model in order to simulate typical mistakes which could be made if binaries were either neglected or not properly taken into account.

Since the photometric method consists in considering all binary stars as single by assuming their lack of resolution, the resulting mass $M_{phot}$ should be underestimated with respect to the theoretical mass $M_{th}$. However, this scenario occurs only in Model B and Model C, where the initial binary fraction is high, for in Model A $M_{phot} > M_{th}$: this happens because the influence of single stars, which tend to enhance the total cluster mass due to the adopted mass-luminosity relation, prevails on the binary one. Instead, the isochrone fitting method, relying on isochrones to derive the mass of single stars and employing magnitude intervals to calculate that of different-mass-ratio binaries, yields a mass estimate $M_{iso}$ which is overestimated in Model A and Model B, but underestimated in Model C if compared to $M_{th}$. According to the confusion matrix, the former case is due to both the high number of appropriately classified single stars, for which holds the same mass-luminosity relation selected in the photometric method, and the lack of mislabelled binary systems, whereas the opposite occurs in the latter case.

Although both methods have pointed out the Model B is the most accurate and accountable one in regard to the total cluster mass estimate, it is evident that a more careful treatment of binary stars is required in order for better results to be achieved: in fact, even a small fraction of either undetected or mislabelled binaries may lead to definitely wrong values of the total cluster mass.

In addition to this, a more realistic scenario can be accomplished by embedding the simulated open clusters in a tidal field, so that the condition of virial equilibrium is not satisfied anymore: thus the dissolution timescale will be shorter, for a significant number of escaped stars, i.e. stars which have crossed the cluster tidal radius, is expected to be present and contribute to mass loss together with stellar evolution and

strong interactions.
Also, investigating the effects of binary stars in the determination of star cluster dynamical masses via the virial theorem may be intriguing, in response of the fact that binaries tend to inflate the line-of-sight velocity dispersion of the hosting clusters.

Such are the perspectives for future developments of this work.

# Bibliography


[1] S. J. Aarseth. *Gravitational N-Body simulations*. 2010.

[2] S. J. Aarseth and M. Lecar. "Computer simulations of stellar systems." In: *Annual Review of Astronomy and Astrophysics* 13 (Jan. 1975), pp. 1–88.

[3] P. Bianchini et al. "The effect of unresolved binaries on globular cluster proper-motion dispersion profiles". In: *ApJ* 820.1 (Mar. 2016), p. L22.

[4] J. Binney and S. Tremaine. *Galactic dynamics: second edition*. 2008.

[5] O. I. Borodina et al. "Unresolved Binaries and Galactic Clusters' Mass Estimates". In: *ApJ* 874.2 (Mar. 2019), p. 127.

[6] G. Carraro et al. "Updated properties of the old open cluster Melotte 66: searching for multiple stellar populations". In: *A&A* 566 (June 2014), A39.

[7] J. Choi et al. "Mesa Isochrones and Stellar Tracks (MIST). I. solar-scaled models". In: *ApJ* 823 (June 2016), p. 102.

[8] A. Dotter. "MESA Isochrones and Stellar Tracks (MIST) 0: methods for the construction of stellar isochrones". In: *ApJS* 222 (Jan. 2016), p. 8.

[9] M. Gieles, H. Sana, and S. F. Portegies Zwart. "On the velocity dispersion of young star clusters: super-virial or binaries?" In: *MNRAS* 402.3 (Mar. 2010), pp. 1750–1757.

[10] T. G. Hawarden. "The old open cluster Melotte 66". In: *MNRAS* 174 (Feb. 1976), pp. 471–487.

[11] S. J. Hogeveen. "The mass-ratio distribution of spectroscopic binary stars". In: *Ap&SS* 196.2 (Oct. 1992), pp. 299–336.

[12] S. J. Hogeveen. "The mass-ratio distribution of visual binary stars". In: *Ap&SS* 173.2 (Nov. 1990), pp. 315–342.

[13] P. Hut et al. "Binaries in globular clusters". In: *Astronomical Society of the Pacific* 104 (Nov. 1992), p. 981.

[14] J. Ji and J. N. Bregman. "Binary frequencies in a sample of globular clusters. I. methodology and initial results". In: *ApJ* 768.2 (May 2013), p. 158.

[15] T. Kaczmarek, C. Olczak, and S. Pfalzner. "Evolution of the binary population in young dense star clusters". In: *A&A* 528 (Apr. 2011), A144.

[16] P. Khalaj and H. Baumgardt. "The stellar mass function, binary content and radial structure of the open cluster Praesepe derived from PPMXL and SDSS data". In: *MNRAS* 434.4 (Oct. 2013), pp. 3236–3245.
[17] C. Korntreff, T. Kaczmarek, and S. Pfalzner. "Towards the field binary population: influence of orbital decay on close binaries". In: *A&A* 543 (July 2012), A126.
[18] M. B. N. Kouwenhoven and R. de Grijs. "How do binaries affect the derived dynamical mass of a star cluster?" In: *Ap&SS* 324.2-4 (Dec. 2009), pp. 171–176.
[19] M. B. N. Kouwenhoven et al. "Exploring the consequences of pairing algorithms for binary stars". In: *A&A* 493.3 (Jan. 2009), pp. 979–1016.
[20] P. Kroupa. "On the variation of the initial mass function". In: *MNRAS* 322.2 (Apr. 2001), pp. 231–246.
[21] P. Kroupa, C. A. Tout, and G. Gilmore. "The distribution of low-mass stars in the Galactic disc". In: *MNRAS* 262 (June 1993), pp. 545–587.
[22] K. Nitadori and S. J. Aarseth. "Accelerating NBODY6 with graphics processing units". In: *MNRAS* 424.1 (July 2012), pp. 545–552.
[23] R. J. Parker and M. M. Reggiani. "The binary companion mass ratio distribution: an imprint of the star formation process?" In: *MNRAS* 432.3 (July 2013), pp. 2378–2384.
[24] R. J. Parker et al. "Do binaries in clusters form in the same way as in the field?" In: *MNRAS* 397.3 (Aug. 2009), pp. 1577–1586.
[25] B. Paxton et al. "Modules for Experiments in Stellar Astrophysics (MESA)". In: *ApJS* 192 (Jan. 2011), p. 3.
[26] B. Paxton et al. "Modules for Experiments in Stellar Astrophysics (MESA): binaries, pulsations, and explosions". In: *ApJS* 220 (Sept. 2015), p. 15.
[27] B. Paxton et al. "Modules for Experiments in Stellar Astrophysics (MESA): convective boundaries, element diffusion, and massive star explosions". In: *ApJS* 234 (Feb. 2018), p. 34.
[28] B. Paxton et al. "Modules for Experiments in Stellar Astrophysics (MESA): planets, oscillations, rotation, and massive stars". In: *ApJS* 208 (Sept. 2013), p. 4.
[29] H. C. Plummer. "On the problem of distribution in globular star clusters". In: *MNRAS* 71 (Mar. 1911), pp. 460–470.
[30] L. Prisinzano et al. "Luminosity and mass function of Galactic open clusters I. NGC 4815". In: *A&A* 369 (Apr. 2001), pp. 851–861.
[31] Reggiani, M. and Meyer, M. R. "Universality of the companion mass-ratio distribution". In: *A&A* 553 (2013), A124.
[32] A. F. Seleznev. "A method for estimating the mass and luminosity functions of star clusters". In: *Astronomy Reports* 42.2 (Mar. 1998), pp. 153–159.
[33] A. F. Seleznev et al. "On the mass of the Galactic star cluster NGC 4337". In: *MNRAS* 467.3 (June 2017), pp. 2517–2528.
[34] L. Spitzer. *Dynamical evolution of globular clusters*. 1987.

[35] J. E. Tohline. "The origin of binary stars". In: *Annual Review of Astronomy and Astrophysics* 40 (Jan. 2002), pp. 349–385.
[36] V. Trimble. "On the distribution of binary system mass ratios". In: *AJ* 79 (Sept. 1974), p. 967.
[37] K. Zloczewski et al. "Variable stars in the field of the old open cluster Melotte 66". In: *MNRAS* 380.3 (Sept. 2007), pp. 1191–1197.